Scheme 6. Construction of Hexadepsipeptide 7

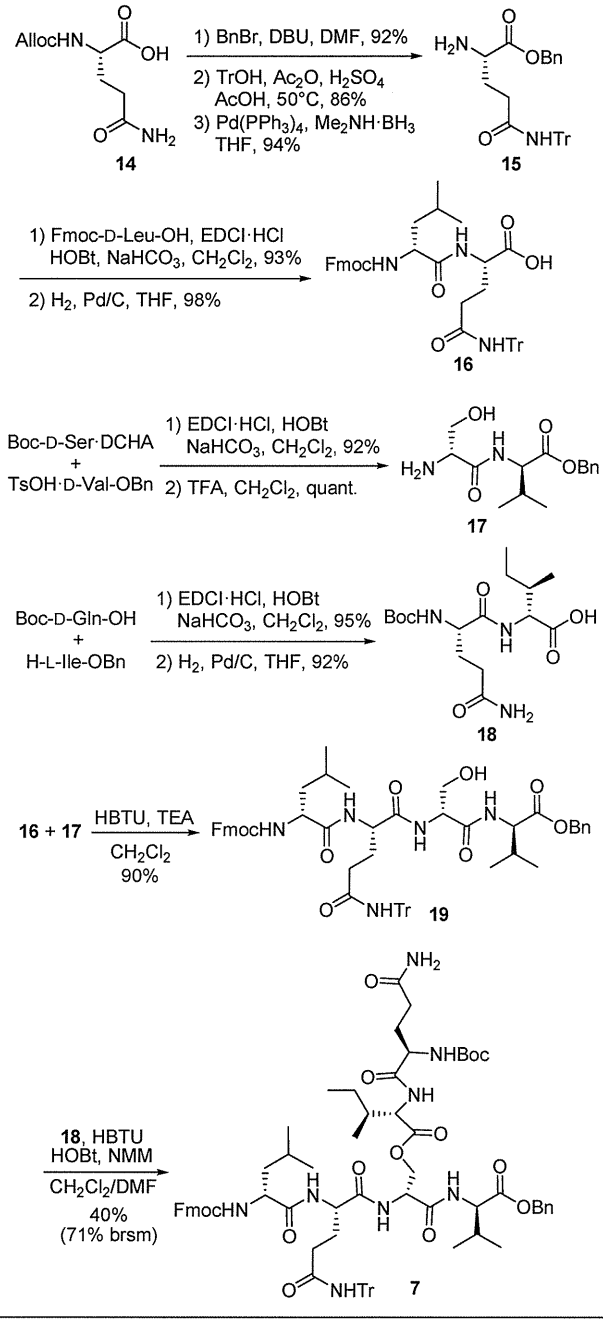

Scheme 7. Synthesis of Decadepsipeptide 6

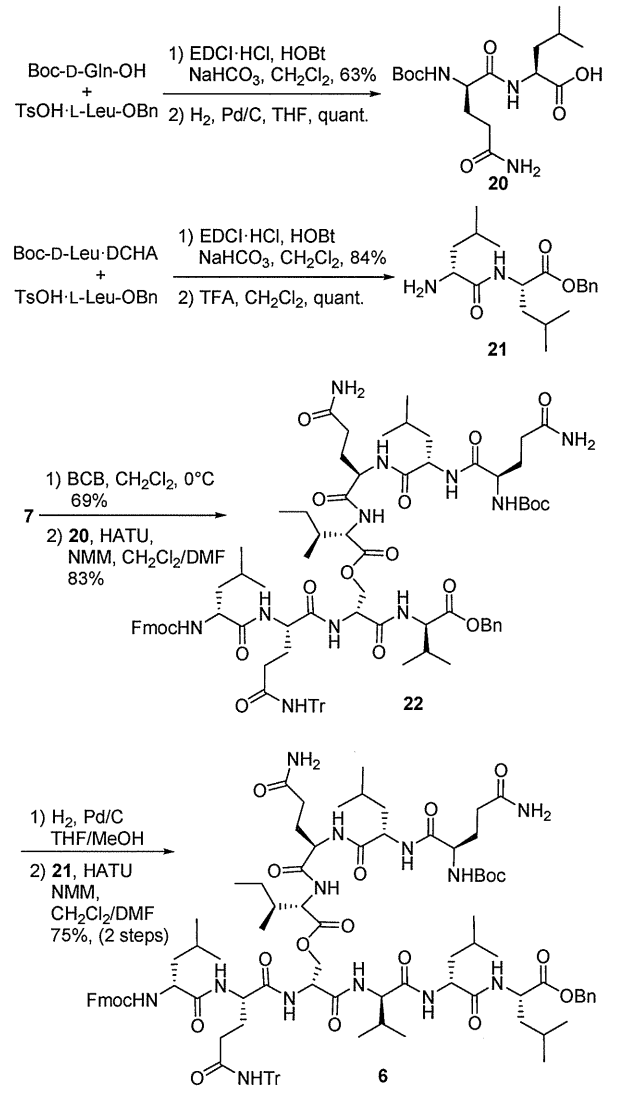

(EDCI), reactive mixed-anhydride activations, Yamaguchi esterification,[20] the Mukaiyama reagent,[21] and the Shiina reagent.[22] An esterification with EDCI, 1-hydroxybenzotriazole (HOBt) and *N*-methylmorpholine (NMM) resulted in low conversion, while the other protocols yielded no detectable product. Finally, esterification of **19** with **18** was successfully achieved in the presence of HBTU, HOBt, and NMM to afford hexadepsipeptide **7** in 40% yield (71% brsm).

With hexadepsipeptide **7** assembled, we turned our attention to the synthesis of decadepsipepide **6** (Scheme 7). Two dipeptides **20** and **21**, components of **6**, were prepared as described below. Condensation of Boc-D-Gln with L-Leu-OBn (63% yield) followed by benzyl ester hydrogenolysis gave the corresponding dipeptide carboxylic acid **20** in quantitative yield. Boc-D-Leu and L-Leu-OBn were coupled (84% yield), and removal of the Boc group under acidic conditions provided the corresponding dipeptide amine **21** in quantitative yield. The next step was the incorporation of these dipeptides into hexadepsipeptide **7**. Selective removal of the Boc group of **7** without affecting the Tr group was accomplished by treatment with *B*-bromocatecholborane (BCB)[23] in CH_2Cl_2 in 69% yield, and the resulting hexadepsipeptide amine was coupled with **20** in the presence of HATU and NMM to afford octadepsipeptide **22** in 83% yield. Next, benzyl ester hydrogenolysis of **22** was performed. However, an unexpected cleavage of the Fmoc group was observed when this reaction was conducted in methanol (MeOH). In the case of another benzyl ester hydrogenolysis that provided dipeptide carboxylic acid **16** (Scheme 6), the Bn group was removed without the cleavage of the Fmoc group in tetrahydrofuran (THF). Octadepsipeptide **22** was difficult to dissolve in a moderately polar aprotic solvent such as THF, while the dipeptide described above dissolved with ease. This problem was resolved by introducing a 3:1 mixture of THF and MeOH as the solvent and adjusting the reaction time to allow complete benzyl ester hydrogenolysis.[24] Removal of the Bn group of **22** in 3:1 THF/MeOH provided the corresponding carboxylic acid. Subsequent coupling with **21** afforded decadepsipeptide **6** in 75% yield over the two steps.

dx.doi.org/10.1021/ja410145x | J. Am. Chem. Soc. XXXX, XXX, XXX–XXX

Having successfully obtained the macrocyclization substrate decadepsipeptide **6**, we next examined the cleavage of the Boc, Bn, and Tr groups and the subsequent intramolecular macrocyclization (Scheme 8). First, the Boc and Tr groups of **6** were removed under acidic conditions to provide the corresponding decadepsipeptide amine. The resulting product was next subjected to benzyl ester hydrogenolysis. However, it proved difficult to remove the benzyl ester selectively without affecting the Fmoc group because the decadepsipeptide amine dissolved in polar protic solvents such as MeOH or mixed solvents of THF/MeOH containing MeOH at a higher rate. Therefore, the deprotection sequence was changed. Benzyl ester hydrogenolysis of **6** proceeded in 1:1 THF/MeOH to provide the corresponding decadepsipeptide carboxylic acid, and then the Boc and Tr groups were removed with trifluoroacetic acid (TFA) in CH_2Cl_2 to afford the macrocyclization precursor.[25] At the stage of macrocyclization, reactions were performed under high-dilution conditions by slow addition of the substrate using a syringe pump in order to prevent the intermolecular reaction. We conducted the macrocyclization reaction with several coupling reagents,[26] including HATU, (benzotriazol-1-yloxy)tris(dimethylamino)-phosphonium hexafluorophosphate (BOP), (benzotriazol-1-yloxy)tripyrrolidinophosphonium hexafluorophosphate (PyBop), and (7-azabenzotriazol-1-yloxy)-tripyrrolidinophosphonium hexafluorophosphate (PyAOP). The protocol using PyAOP and 4-dimethylaminopyridine (DMAP) in DMF was found to promote the closure of the 25-membered ring to afford cyclodepsipeptide **3** in 18% yield over the three steps.

Scheme 8. Synthesis of Cyclodepsipeptide 3

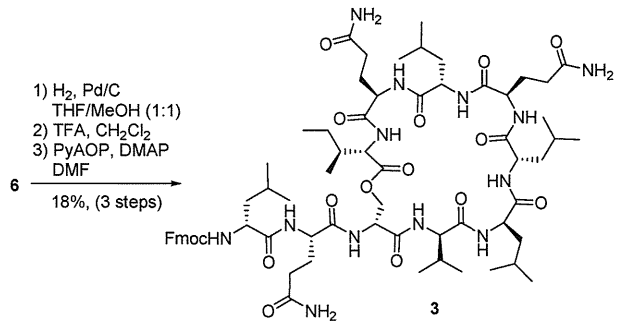

Total Synthesis of MA026. With the two required key segments (side chain **2** and cyclodepsipeptide **3**) in hand, we sought to link them together to accomplish the synthesis of MA026 (**1**) (Scheme 9). Removal of the N-terminal Fmoc group of **3** proceeded with diethylamine in DMF to provide the corresponding cyclodepsipeptide amine **24**. An alternative deprotection with piperidine resulted in the formation of several side products that were difficult to separate from **24**. Benzyl ester hydrogenolysis of **2** and subsequent coupling with amine **24** in the presence of PyAOP and DMAP furnished **25**. Although the deprotection of **2** and **3** gave corresponding

Scheme 9. Synthesis of MA026 (1)

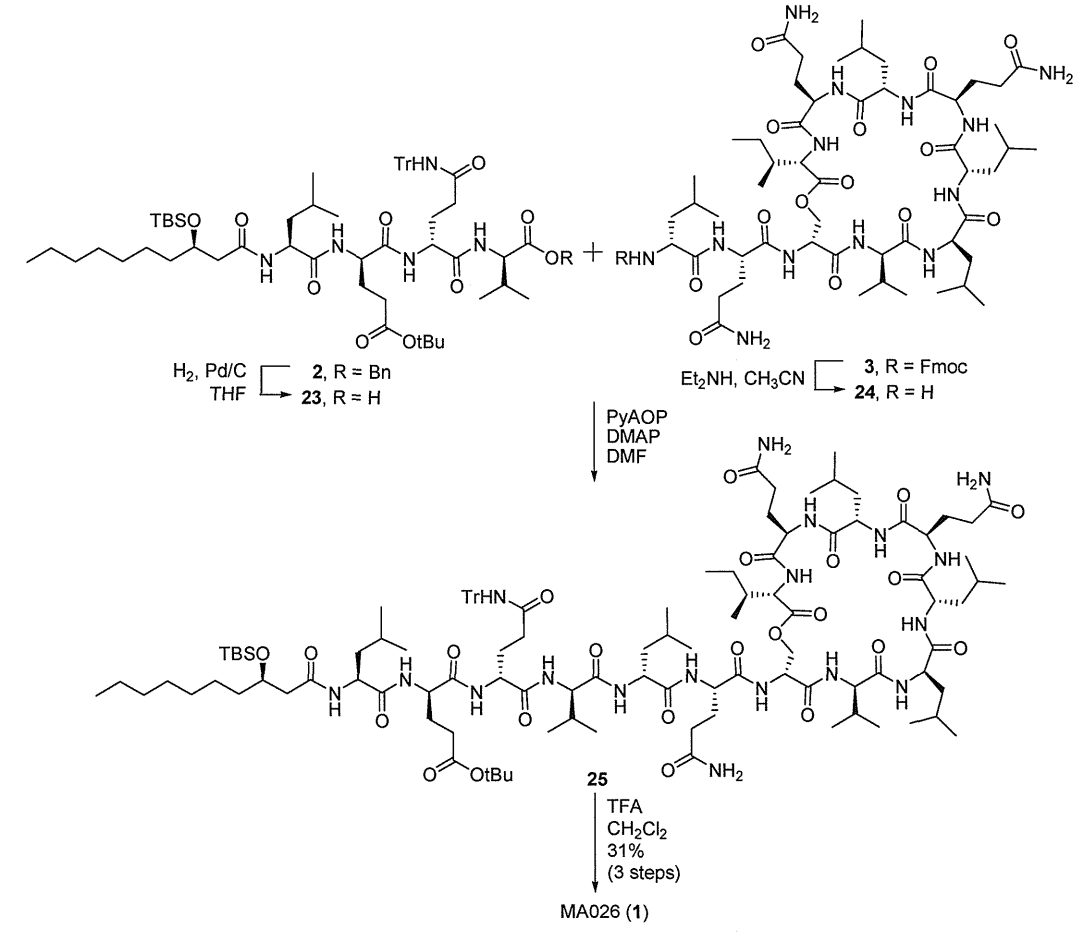

dx.doi.org/10.1021/ja410145x | J. Am. Chem. Soc. XXXX, XXX, XXX–XXX

carboxylic acid **23** and amine **24** in quantitative yield, their coupling did not proceed completely. Finally, a single-step cleavage of the Tr, *t*Bu, and TBS groups in **25** was achieved with TFA. The crude material was purified by reversed-phase HPLC to furnish pure **1** in 31% yield over the three steps. Analysis of synthetic **1** by ^{1}H and ^{13}C NMR spectroscopy, along with other spectroscopic data, showed it to be identical to the natural product.

Anti-HCV Activity of MA026 (1). MA026 shows antiviral activity against both IHNV and HCV. Given the fact that IHNV and HCV share a common entry process,[27,28] we reasoned that MA026 might inhibit the HCV entry process, which consists of cell binding, postcell binding, and endocytosis. On the basis of this prediction, we studied the anti-HCV activity of MA026 by measuring the HCV infectivity to determine whether MA026 inhibits the HCV entry process. Moreover, we compared the anti-HCV activity of synthetic **1** with that of the natural product (Figure 2).[29] Infectious HCV

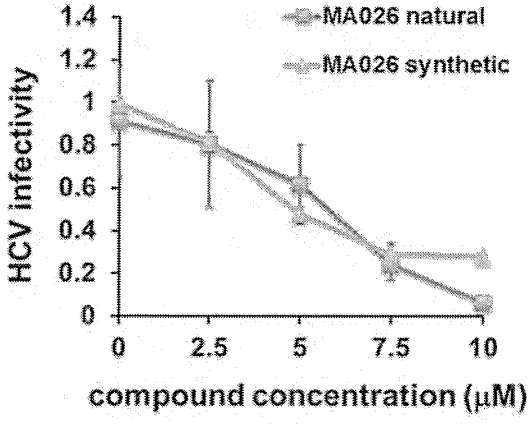

Figure 2. Evaluation of the anti-HCV activity of synthetic and natural **1**. The normalized infectivity was calculated as the HCV infectivity divided by the cell viability.

particles were pretreated with compounds for 1 h and infected into Huh-7.5.1 cells for 4 h. After residual virus and the test compound were washed out, cells were further cultured with growth medium in the absence of the compound for 72 h. The infectivity of HCV in the medium was quantified, and half-maximal inhibitory concentration (IC_{50}) values of the compounds were determined. In this assay, cells were exposed to the test compound only before and during HCV infection. Therefore, this pretreatment procedure could evaluate the potency of the test compound to inhibit the HCV entry process into the host cells. As shown in Figure 2, both synthetic **1** and the authentic natural product suppressed HCV infection into the host cells in a dose-dependent manner (IC_{50} = 4.39 and 4.68 μM, respectively). Moreover, incubation in the presence of these compounds did not induce significant cytotoxicity within the concentration range used in these tests (Figure S1 in the Supporting Information). Thus, our data suggest that MA026 inhibits HCV infection by blocking the entry process. Phage display screening with immobilized MA026 and SPR binding analyses suggested claudin-1 as a candidate target for the anti-HCV activity of MA026.

To identify MA026 binding proteins, we applied a chemical biology approach and performed phage display screening.[30] Previously, we used phage display analyses to elucidate a novel mechanism of HCV replication by identifying the target protein of cyclosporin A.[31] Here we employed the same strategy to identify the target of MA026. MA026 was first immobilized on photoaffinity resin containing a photoactive diazirine group that we previously developed (Scheme S1 in the Supporting Information).[32,33] The mixture of photoafiinity resin and MA026 was irradiated with UV light. The highly reactive carbene induced by UV irradiation reacted with MA026, resulting in the production of immobilized MA026 in a nonspecific manner. Having prepared the MA026-immobilized resin, we then performed phage display screening using a random phage library displaying random peptides composed of 15 amino acids.[34] The phage display screening method is a powerful tool for identifying binding proteins of specific ligands. In this method, the phage library displaying peptides on phage particles (Input) was incubated with either MA026-immobilized resin or control resin (Bind) (Figure 3A and Figure S2A in the Supporting Information). Unbound phage particles were removed by washing (Selection). Phage particles bound to the MA026-immobilized resin were then eluted (Elute) and amplified in *Escherichia coli* (Amplify). The recovered phage clones (Input) were subsequently subjected to the next round of biopanning. Upon iteration of the biopanning cycles, the recovery rate of eluted phage clones compared with Input increased (Figure S2B). The relative enrichment of phage particles bound to MA026-immobilized resin was the highest upon the elution from the fourth round of biopanning (Figure 3B). Therefore, we randomly picked 27 single phage clones from the fourth-round elution. The sequence of peptides displayed on the phage particles, which were responsible for interaction with MA026, were determined from the DNA sequences of the corresponding phage vectors (Table S1 in the Supporting Information). Multiple sequence alignment analyses using CLUSTALW[35] indicated that peptides 1, 3, 10, 19, and 24 shared homology (Figure S3). Among them, we found the peptide sequence VFDSLL, a partially homologous sequence. We then searched the protein database using BLAST[36] to find proteins that showed similarities to the VFDSLL sequence. A single protein that includes the VFDSLL sequence, claudin-1 (CLDN1), was identified in the NCBI database. CLDN1 is highly expressed in the liver and plays an important role during the postcell binding process of HCV entry.[37]

On the basis of this knowledge and the result of phage display screenings followed by CLUSTALW and BLAST analyses, we proposed a hypothesis that MA026 might interact with CLDN1 and thereby suppress HCV infection. To confirm the interaction between CLDN1 and MA026, we performed SPR binding analyses using recombinant CLDN1 protein with an N-terminal glutathione S-transferase tag (CLDN1-GST). CLDN1-GST, or GST itself as a negative control, was first immobilized on a sensor chip of the SPR biosensor (Biacore 3000), and MA026 samples at different concentrations were then injected over the immobilized proteins.[38] The SPR data (Figure 3C) were subsequently analyzed to determine the dissociation constant (K_D). Our results showed a specific dose-dependent binding response of MA026 with CLDN1-GST (K_D = 2.5 × 10^{-6} M). By contrast, the response with GST itself was significantly weaker (K_D = 4.0 × 10^{-5} M). These results indicate a specific interaction between MA026 and recombinant CLDN1 protein.

The process of HCV entry into human hepatocytes requires the interaction of HCV glycoproteins E1 and E2 with host

dx.doi.org/10.1021/ja410145x | J. Am. Chem. Soc. XXXX, XXX, XXX–XXX

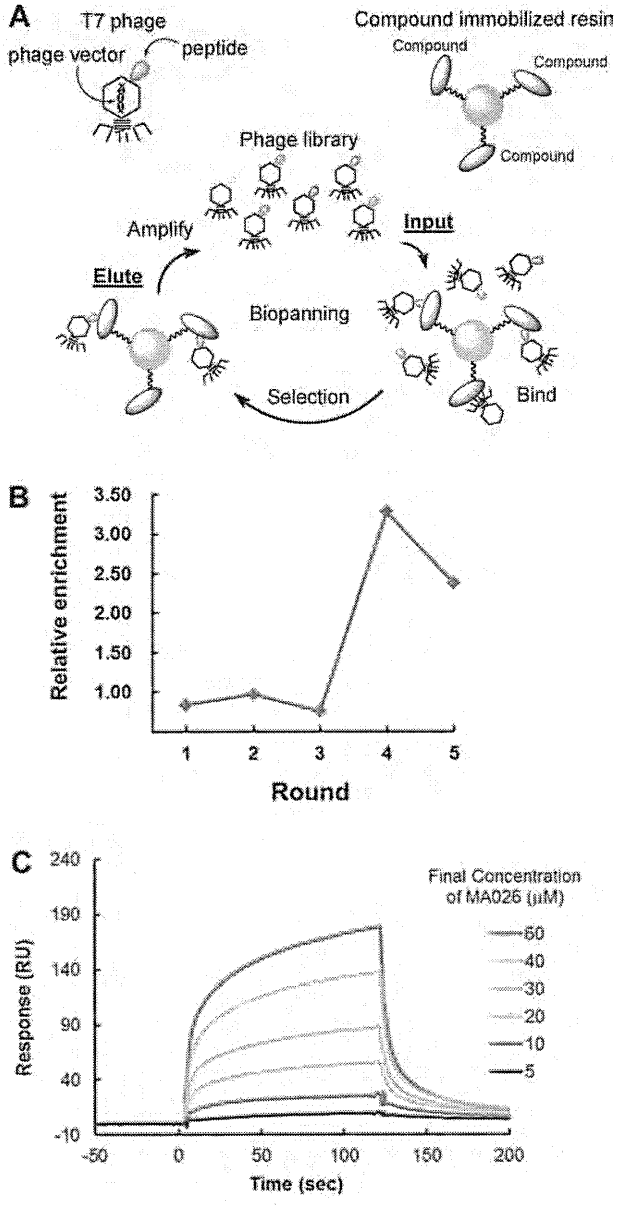

Figure 3. Phage display screenings and SPR analyses. (A) Procedure of phage display screening. (B) Relative enrichment of phage particles bound to MA026-immobilized resin. Relative enrichment was determined as the ratio of phage titer of elution from MA026-imobilized resin to phage titer of elution from control resin. (C) SPR analysis of binding between CLDN1-GST and MA026. Response units (RU) were calculated by subtracting the background response measured on the control flow cell from the response with the MA026 flow cell.

receptors, including tetraspanin CD81 and the high density lipoprotein receptor scavenger receptor class B type I (SR-BI).[39] It was reported that these two receptors are not sufficient for HCV entry and that more host proteins are involved.[40] CLDN1 is a transmembrane protein and belongs to a family of tight junction proteins that act as a barrier in cellular permeability.[41] It has been proposed that during the course of HCV entry, CLDN1 interacts with CD81 and influences the cell entry process, including endocytosis.[42] Although direct binding between HCV particles and CLDN1 has not been conclusively demonstrated, it has been shown that monoclonal anti-CLDN1 antibodies prevent HCV infection.[43] The peptide sequence VFDSLL, which is likely to interact with MA026, is conserved in the first extracellular loop (EL1) of CLDN1, and this loop is required for HCV entry.[37] The SPR analysis showed an interaction between MA026 and CLDN1-GST, and this result supports our hypothesis that MA026 might interact with CLDN1 and thereby prevent CLDN1 from interacting with CD81 and the HCV particle.

CONCLUSIONS

The first total synthesis of MA026 was achieved in the solution phase with two key segments: side chain **2** and cyclodepsipeptide **3**. The construction of side chain **2** was accomplished with good efficiency by coupling of fatty acid moiety **4** with tripeptide **5**. In the preparation of macrocyclization substrate decadepsipeptide **6**, an appropriate choice of solvent was required to avoid the cleavage of the N-terminal Fmoc group through hydrogenolysis reactions. The key macrocyclization of the decadepsipeptide at L-Leu^{10}-D-Gln^{11} was accomplished with PyAOP to afford **3**. This convergent modular synthetic route will be useful for the synthesis of a series of MA026 derivatives that will facilitate structure–activity relationship studies. Moreover, xantholysin A, an analogue of MA026, could be synthesized via this route once the stereochemistry is determined.

The anti-HCV activities of synthetic **1** and the authentic natural product were assessed and found to be similar. In this assay, the cells were exposed to the test compound only before and during HCV infection and then subsequently cultured in the absence of the test compound until sampling. Our results suggest that MA026 might inhibit the early step of HCV infection, including the cell entry process, rather than the following steps such as RNA replication and viral assembly and release. Phage display screenings were performed using MA026-immobilized resin and a random phage library. As the biopanning cycle was repeated, the ratio of phage clones bound to MA026 increased. We randomly picked 27 single phage clones and determined the peptide sequences displayed on the phage particles. From the results of multiple sequence alignment analyses using CLUSTALW, we found VFDSLL, a partially homologous peptide sequence. A BLAST search identified CLDN1 as a protein bearing the VFDSLL sequence. This protein plays an important role in the HCV entry process. The specific interaction between MA026 and recombinant CLDN1 protein was then confirmed by SPR analyses. Because the VFDSLL sequence is conserved in EL1 of CLDN1, we speculate that MA026 might interact with EL1 of CLDN1 and thereby interrupt HCV entry into the host cell.

Further investigations to develop an improved synthetic route that provides more efficient access to analogues and to reveal the detailed mechanism of the anti-HCV activity of MA026 are currently underway and will be disclosed in due course.

ASSOCIATED CONTENT

Supporting Information

Experimental procedures and analytical data for new compounds. This material is available free of charge via the Internet at http://pubs.acs.org.

AUTHOR INFORMATION

Corresponding Author

sugawara@rs.noda.tus.ac.jp

dx.doi.org/10.1021/ja410145x | J. Am. Chem. Soc. XXXX, XXX, XXX–XXX

Notes

The authors declare no competing financial interest.

■ ACKNOWLEDGMENTS

We are grateful for the financial support of Toyo Suisan Kaisha, LTD., ADEKA Corporation, and a Sasakawa Scientific Research Grant from The Japan Science Society.

■ REFERENCES

(1) Ishima, M.; Yoshida, T.; Yamazaki, T.; Sugawara, F.; Hatta, K.; Shimojoe, M.; Masaki, K. PCT WO 02/062831, 2002.
(2) (a) Liang, T. J.; Jeffers, L. J.; Reddy, K. R.; Medina, M. D.; Parker, I. T.; Cheinquer, H.; Idrovo, V.; Rabassa, A.; Schiff, E. R. *Hepatology* **1993**, *18*, 1326–1333. (b) Lauer, G. M.; Walker, B. D. *N. Engl. J. Med.* **2001**, *345*, 41–52.
(3) Poynard, T.; Yuen, M. F.; Ratzin, V.; Lai, C. L. *Lancet* **2003**, *362*, 2095–2100.
(4) Tai, A. W.; Chung, R. T. *J. Hepatol.* **2009**, *50*, 412–420.
(5) Joyce, M. A.; Tyrrell, D. L. *J. Microbes Infect.* **2010**, *12*, 263–271.
(6) Wakita, T.; Pietschmann, T.; Kato, T.; Date, T.; Miyamoto, M.; Zhao, Z.; Murthy, K.; Habermann, A.; Kräusslich, H.; Mizokami, M.; Bartenschlager, R.; Liang, T. J. *Nat. Med. (New York, NY, U.S.)* **2005**, *11*, 791–796.
(7) Kim, H. J.; Oseko, N.; Nishizawa, T.; Yoshimizu, M. *Dis. Aquat. Org.* **2009**, *83*, 105–113.
(8) Wolf, K. Infectious Hematopoietic Necrosis. In *Fish Viruses and Fish Viral Disease*; Wolf, K., Ed.; Cornell University Press: Ithaca, NY, 1988; pp 83–114.
(9) Winton, J. R. *Annu. Rev. Fish Dis.* **1991**, *1*, 83–93.
(10) (a) Stolze, S. C.; Kaiser, M. *Molecules* **2013**, *18*, 1337–1367. (b) Andavan, G. S. B.; Lemmens-Gruber, R. *Mar. Drugs* **2010**, *8*, 810–834.
(11) Li, W.; Rokni-Zadeh, H.; Vleeschouwer, M. D.; Ghequire, M. G. K.; Sinnaeve, D.; Xie, G.; Rozenski, J.; Madder, A.; Martins, J. C.; Mot, R. D. *PLoS One* **2013**, *8*, No. e62946.
(12) Davies, J. S. *J. Pept. Sci.* **2003**, *9*, 471–501.
(13) Jiang, W.; Wanner, J.; Lee, R. J.; Bounaud, P.; Boger, D. L. *J. Am. Chem. Soc.* **2003**, *125*, 1877–1887.
(14) Alcohol **8** was synthesized by the asymmetric samarium-Reformatsky reaction of *n*-octylaldehyde with Evans' chiral 3-(2-bromoacetyl)-2-oxazolidinone. The overall yield of **8** was 48% over the two steps from Evans' chiral oxazolidinone. See: Fukuzawa, S.; Matsuzawa, H.; Yoshimitsu, S. *J. Org. Chem.* **2000**, *65*, 1702–1706.
(15) Boger, D. L.; Lee, R. J.; Bounaud, P.; Meier, P. *J. Org. Chem.* **2000**, *65*, 6770–6772.
(16) Gomez-Martinez, P.; Dessolin, M.; Guibé, F.; Albericio, F. *J. Chem. Soc., Perkin Trans. 1* **1999**, *1*, 2871–2874.
(17) Although hydrogenolysis of the benzyl ester in **4** gave carboxylic acid **12** in 94% yield, the cleavage of the Fmoc group in **5** gave amine **13** and some side products. See the Supporting Information for the synthesis of side chain **2**.
(18) Stevens, C. M.; Watanabe, R. *J. Am. Chem. Soc.* **1950**, *72*, 1877–1887.
(19) The preparation of Boc-D-Ser·DCHA is described in the Supporting Information.
(20) Inanaga, J.; Hirata, K.; Saeki, H.; Katsuki, T.; Yamaguchi, M. *Bull. Chem. Soc. Jpn.* **1979**, *52*, 1989–1993.
(21) Narasaka, K.; Maruyama, K.; Mukaiyama, T. *Chem. Lett.* **1978**, 885–888.
(22) (a) Shiina, I.; Ibuka, R.; Kubota, M. *Chem. Lett.* **2002**, 286–287. (b) Shiina, I.; Kubota, M.; Ibuka, R. *Tetrahedron Lett.* **2002**, *43*, 7535–7539.
(23) Boeckman, R. K, Jr.; Potenza, J. C. *Tetrahedron Lett.* **1985**, *26*, 1411–1414.
(24) In addition to the ratio of THF and MeOH, the amount of Pd/C was important to avoid the cleavage of the Fmoc group. The amount of Pd/C should be less than or equal to 0.1 equiv.
(25) The benzyl ester hydrogenolysis of **6** in 1:1 THF/MeOH gave the desired decadepsipeptide carboxylic acid, but the crude product included some peptides without the Fmoc group.
(26) (a) Han, S.; Kim, Y. *Tetrahedron* **2004**, *60*, 2447–2467. (b) Valeur, E.; Bradley, M. *Chem. Soc. Rev.* **2009**, *38*, 606–631.
(27) Liu, H.; Liu, Y.; Liu, S.; Pang, D.; Xiao, G. *J. Virol.* **2011**, *85*, 6252–6262.
(28) Blanchard, E.; Belouzard, S.; Goueslain, L.; Wakita, T.; Dubuisson, J.; Wychowski, C.; Rouillé, Y. *J. Virol.* **2006**, *80*, 6964–6972.
(29) Zhong, J.; Gastaminza, P.; Cheng, G.; Kapadia, S.; Kato, T.; Burton, D. R.; Wieland, S. F.; Uprichard, S. L.; Wakita, T.; Chisari, F. V. *Proc. Natl. Acad. Sci. U.S.A.* **2005**, *102*, 9294–9299.
(30) Smith, G. P.; Petrenko, V. A. *Chem. Rev.* **1997**, *97*, 391–410.
(31) Morohashi, K.; Sahara, H.; Watashi, K.; Iwabata, K.; Sunoki, T.; Kuramochi, K.; Takakusagi, K.; Miyashita, H.; Sato, N.; Tanabe, A.; Shimotohno, K.; Kobayashi, S.; Sakaguchi, K.; Sugawara, F. *PLoS One* **2011**, *6*, No. e18285.
(32) (a) Kanoh, N.; Honda, K.; Simizu, S.; Muroi, M.; Osada, H. *Angew. Chem., Int. Ed.* **2005**, *44*, 3559–3562. (b) Kuramochi, K.; Haruyama, T.; Takeuchi, R.; Sunoki, T.; Watanabe, M.; Oshige, M.; Kobayashi, S.; Sakaguchi, K.; Sugawara, F. *Bioconjugate Chem.* **2005**, *16*, 97–104.
(33) We used the natural product to prepare MA026-immobilized resin.
(34) Kusayanagi, T.; Tsukuda, S.; Shimura, S.; Manita, D.; Iwakiri, K.; Kamisuki, S.; Takakusagi, Y.; Takeuchi, T.; Kuramochi, K.; Nakazaki, A.; Sakaguchi, K.; Kobayashi, S.; Sugawara, F. *Bioorg. Med. Chem.* **2012**, *20*, 6248–6255.
(35) Thompson, J. D.; Higgins, D. G.; Gibson, T. J. *Nucleic Acids Res.* **1994**, *22*, 4673–4680.
(36) Altschul, S. F.; Madden, T. L.; Schäffer, A. A.; Zhang, J.; Zhang, Z.; Miller, W.; Lipman, D. J. *Nucleic Acids Res.* **1997**, *25*, 3389–3402.
(37) Evans, M. J.; von Hahn, T.; Tscherne, D. M.; Syder, A. J.; Panis, M.; Wölk, B.; Hatziioannou, T.; McKeating, J. A.; Bieniasz, P. D.; Rice, C. M. *Nature* **2007**, *446*, 801–805.
(38) In SPR analyses, we used the MA026 natural product.
(39) (a) Pileri, P.; Uematsu, Y.; Compagnoli, S.; Galli, G.; Falugi, F.; Petracca, R.; Weiner, A. J.; Houghton, M.; Rosa, D.; Grandi, G.; Abrignani, S. *Science* **1998**, *282*, 938–941. (b) Scarselli, E.; Ansuini, H.; Cerino, R.; Roccasecca, R. M.; Acali, S.; Filocamo, G.; Traboni, C.; Nicosia, A.; Cortese, R.; Vitelli, A. *EMBO J.* **2002**, *21*, 5017–5025.
(40) Bartosch, B.; Cosset, F. L. *Virology* **2006**, *348*, 1–12.
(41) Van Itallie, C. M.; Anderson, J. M. *Annu. Rev. Physiol.* **2006**, *68*, 403–429.
(42) Brazzoli, M.; Bianchi, A.; Filippini, S.; Weiner, A.; Zhu, Q.; Pizza, M.; Crotta, S. *J. Virol.* **2008**, *82*, 8316–8329.
(43) Krieger, S. E.; Zeisel, M. B.; Davis, C.; Thumann, C.; Harris, H. J.; Schnober, E. K.; Mee, C.; Soulier, E.; Royer, C.; Lambotin, M.; Grunert, F.; Thi, V. L. D.; Dreux, M.; Cosset, F.; McKeating, J. A.; Schuster, C.; Baumert, T. F. *Hepatology* **2010**, *51*, 1144–1157.

Journal of General Virology (2014), **95**, 60–65 DOI 10.1099/vir.0.058008-0

Short Communication

Production of single-round infectious chimeric flaviviruses with DNA-based Japanese encephalitis virus replicon

Ryosuke Suzuki,[1]† Tomohiro Ishikawa,[2]† Eiji Konishi,[3] Mami Matsuda,[1] Koichi Watashi,[1] Hideki Aizaki,[1] Tomohiko Takasaki[4] and Takaji Wakita[1]

Correspondence
Ryosuke Suzuki
ryosuke@nih.go.jp
Eiji Konishi
ekon@biken.osaka-u.ac.jp

[1]Department of Virology II, National Institute of Infectious Diseases, Toyama 1-23-1, Shinjuku-ku, Tokyo 162-8640, Japan

[2]Department of Microbiology, Dokkyo Medical University School of Medicine, 880 Kitakobayashi, Mibu-machi, Shimotsuga-gun, Tochigi, 321-0293, Japan

[3]BIKEN Endowed Department of Dengue Vaccine Development, Faculty of Tropical Medicine, Mahidol University, 420/6 Ratchawithi Road, Ratchahewi, Bangkok 10440, Thailand

[4]Department of Virology I, National Institute of Infectious Diseases, Toyama 1-23-1, Shinjuku-ku, Tokyo 162-8640, Japan

A method for rapid production of single-round infectious particles (SRIPs) of flavivirus would be useful for viral mutagenesis studies. Here, we established a DNA-based production system for SRIPs of flavivirus. We constructed a Japanese encephalitis virus (JEV) subgenomic replicon plasmid, which lacked the C-prM-E (capsid–pre-membrane–envelope) coding region, under the control of the cytomegalovirus promoter. When the JEV replicon plasmid was transiently co-transfected with a JEV C-prM-E expression plasmid into 293T cells, SRIPs were produced, indicating successful *trans*-complementation with JEV structural proteins. Equivalent production levels were observed when C and prM–E proteins were provided separately. Furthermore, dengue types 1–4, West Nile, yellow fever or tick-borne encephalitis virus prM-E proteins could be utilized for production of chimaeric flavivirus SRIPs, although the production was less efficient for dengue and yellow fever viruses. These results indicated that our plasmid-based system is suitable for investigating the life cycles of flaviviruses, diagnostic applications and development of safer vaccine candidates.

Received 1 August 2013
Accepted 3 October 2013

Japanese encephalitis virus (JEV) is the leading cause of viral encephalitis with severe mortality in eastern and south-eastern Asia, and is estimated to be responsible for 67 900 cases annually, mostly in children (Campbell *et al.*, 2011). The virus is transmitted by *Culex* mosquito vectors between pigs and/or wild birds, and humans and horses are thought to be dead-end hosts. JEV is a member of the genus *Flavivirus* within the family *Flaviviridae*, which includes dengue virus (DENV), West Nile virus (WNV), yellow fever virus (YFV) and tick-borne encephalitis virus (TBEV). JEV is an enveloped single-stranded positive-sense RNA virus with an 11 kb genome that is translated as a single large polyprotein. The polyprotein is co-translationally cleaved by host and viral proteases into three structural proteins – capsid (C), pre-membrane (prM) and envelope (E) – and seven non-structural (NS) proteins (Sumiyoshi *et al.*, 1987).

For several flaviviruses, subgenomic replicons, which lack structural protein genes but can replicate in cells, have been constructed (Khromykh & Westaway, 1997; Pang *et al.*, 2001; Shi *et al.*, 2002). In addition, the expression of viral structural proteins in cells harbouring replicon RNA has been shown to produce single-round infectious particles (SRIPs), which are infectious, but progeny viruses cannot be spread from the infected cells, as the packaged genome lacks structural protein genes (Gehrke *et al.*, 2003; Jones *et al.*, 2005; Khromykh *et al.*, 1998; Ng *et al.*, 2007; Scholle *et al.*, 2004; Yun *et al.*, 2009). Furthermore, *trans*-packaging of replicons by the prM-E proteins from heterologous flaviviruses have been reported (Ansarah-Sobrinho *et al.*, 2008; Yoshii *et al.*, 2008).

A method for rapidly producing SRIPs of flaviviruses would be useful for viral mutagenesis studies, diagnostic applications and the production of vaccines with reduced

†These authors contributed equally to this paper.

One supplementary figure is available with the online version of this paper.

risk of infection. In this study, to establish a DNA-based production system for SRIPs, we constructed a JEV subgenomic replicon plasmid, which lacked the C-prM-E coding region, under the control of the cytomegalovirus (CMV) promoter. As DNA-based replicons can be transfected directly into eukaryotic cells without *in vitro* transcription, SRIPs can be rapidly produced by co-transfection with structural protein-expression plasmids.

In order to generate a subgenomic replicon from the JEV Nakayama strain (McAda *et al.*, 1987), viral RNA was extracted from infected Vero cells, reverse transcribed into cDNA and amplified in individual dsDNA fragments containing T7 RNA polymerase promoter and hepatitis delta virus ribozyme (HDV-RZ) as shown in Fig. 1(a). For deletion of the C-prM-E region, a synthetic antisense oligonucleotide was used to add a *Bsp*TI site at codons 17–18 of the C-coding region following the cyclization sequence, and a sense oligonucleotide was designed that added the *Bsp*TI site before the C-terminal transmembrane domain, which consists of 30 aa of the E protein coding sequence, in order to permit ligation of C to NS1. The five individual fragments required to produce a replicon-length cDNA were readily assembled into the low-copy-number plasmid pACYC177, designated pJEVrep#97. Replication of *in vitro*-transcribed RNAs derived from the plasmid was confirmed in RNA-transfected cells (data not shown). Next, to construct a DNA-based replicon plasmid, the T7 RNA polymerase promoter was replaced with the CMV promoter, and the simian virus 40 polyadenylation signal was inserted downstream of the HDV-RZ; the resulting plasmid was designated pCMV-JErep (Fig. 1a). pCMV-JErep-fs, which contains a frameshift mutation through a 4 nt insertion upstream of the GDD motif of RNA-dependent RNA polymerase in NS5, was also constructed as a negative control with no replication activity. To characterize the replication activity of the plasmid-derived replicon, 293T cells were transfected with plasmids as described previously (Suzuki *et al.*, 2013). Indirect immunofluorescence with an anti-dsRNA antibody showed positive staining in the cytoplasm of cells transfected with pCMV-JErep plasmid or infected with JEV Nakayama strain, whereas no signal was detected in the cells transfected with pCMV-JErep-fs, indicating the ability of viral RNAs transcribed intracellularly from the plasmid pCMV-JErep to replicate in cells (Fig. 1b). It should be noted that NS1 protein was detected in the cytoplasm of cells transfected with both pCMV-JErep and pCMV-JErep-fs.

We also constructed expression plasmids for JEV C-E, mature C consisting of 105 aa, and prM-E, which we designated pCAG-JECE, pCAG-JEC and pCAG-JEprME, respectively (Fig. 2a). To reduce sequence homology and intergenomic recombination potential with the truncated C and E genes in the subgenomic replicon, 21 nt mutations were incorporated into the 5′ region of the C gene and 3′ region of the E gene. These changes also include two nucleotides in the conserved 5′ cyclization sequence (CS) (Hahn *et al.*, 1987; Khromykh *et al.*, 2001), producing a sequence that was non-complementary to the 3′ CS of the replicon genome, thereby preventing replication of a recombinant genome. To produce SRIPs of JEV, 293T cells were transfected with a mixture of two (pCMV-JErep and pCAG-JECE) or three (pCMV-JErep, pCAG-JEC and pCAG-JEprME) plasmids. The infectivity of SRIPs was determined by inoculating the culture supernatant of transfected cells into Vero cells, followed by immunostaining with anti-NS1 antibody. 293T cells produced a titre of 6.9×10^5 IU ml^{-1} (Fig. 2b) or 7.9×10^5 IU ml^{-1} (Fig. 2c) 3 days after transfection with two or three plasmids, respectively. In contrast, no infectious particles were detected in the supernatant when one of the two or three plasmids was omitted or the replicon containing a frameshift mutation was introduced. The production levels of SRIPs from cells transfected with two or three plasmids were similar, as shown in Fig. 2(d).

In order to confirm that the SRIPs have only single-round infectivity potential, Vero cells were inoculated with medium harvested from 293T cells transfected with replicon and structural protein plasmids, and were examined for antigen-positive cells. SRIPs were demonstrated to be infectious in the first round (Fig. 3a). However, no antigen-positive cells were observed in a second round, in which the supernatants of the cells infected with SRIPs were transferred to naive Vero cells (Fig. 3a). As a control, supernatant from JEV-infected cells produced antigen-positive cells in second-round infection.

We then evaluated whether the SRIPs could be used in neutralization tests instead of infectious live virus by using anti-JEV sera raised in rabbits as a representative antibody. Serial fourfold dilutions of serum were mixed with aliquots of SRIPs or virus of equivalent infectivity. The virus–antibody mixture was incubated for 1 h at room temperature, followed by titration for infectivity on Vero cell monolayers in a 96-well plate. The neutralizing activity of each antibody dilution was expressed as a percentage of the infectivity obtained with the control, which was tested in the absence of any serum. Infection with SRIPs and JEV Nakayama strain were similarly neutralized by anti-JEV antibody in a dose-dependent manner, although normal serum did not affect infection with SRIPs and JEV (Fig. 3b).

Next, to examine whether SRIPs derived from other flaviviruses could be generated using our plasmid-based method, we used prM-E expression plasmids for the following viruses: DENV1, Mochizuki strain; DENV2, New Guinea C strain; DENV3, H87 strain; DENV4, H241 strain (Konishi *et al.*, 2006); WNV, NY99-6922 strain (Ishikawa *et al.*, 2007); YFV, 17D strain; and TBEV, Oshima 5-10 strain (Yoshii *et al.*, 2003). Detection of each E protein in cells transfected with prM-E expression plasmids by immunofluorescence revealed indistinguishable efficiency of transfection as shown in Fig. S1 (available in JGV Online). Efficient production of chimaeric flavivirus SRIPs by co-transfection with JEV C and JEV replicons was achieved for

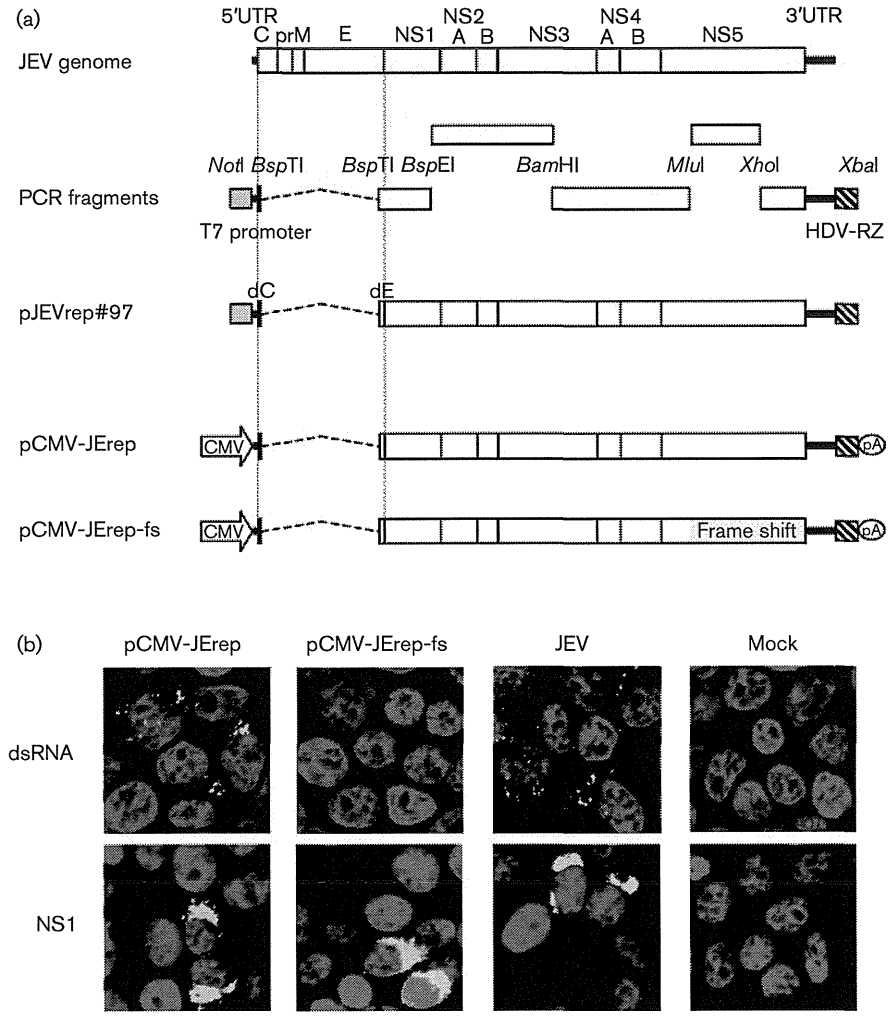

Fig. 1. (a) Schematic representation of the position of the JEV genome showing restriction enzymes sites (*NotI*, *BspTI*, *BspEI*, *BamHI*, *MluI*, *XhoI* and *XbaI*), fragments used to assemble for replicon construction, position of the T7 promoter, CMV promoter (CMV), HDV-RZ and polyadenylation signal (pA). (b) 293T cells were transfected with the indicated plasmids or were infected or mock-infected with JEV. Two days post-transfection or post-infection, cells were fixed and permeabilized as described previously (Suzuki *et al.*, 2013). Samples were then incubated with anti-dsRNA antibody (J2; English & Scientific Consulting) or anti-NS1 antibody (2D5; Konishi *et al.*, 2004). Green signals were obtained with Alexa-Fluor-488-labelled goat anti-mouse IgG secondary antibody (Invitrogen). Cell nuclei were counterstained with DAPI.

WNV and TBEV, although production of SRIPs was less efficient for DENV1-4 and YFV (Fig. 3c).

It is curious that TBEV prM-E protein can be utilized efficiently for assembly of SRIPs in combination with the JEV C protein and replicon RNA producing equivalent titres to JEV and WNV, as TBEV is a tick-borne virus and is classified as a distinct serogroup from JEV. In contrast, production of DENV- and YFV-SRIPs was less efficient. The low infectious titre of SRIPs containing at least dengue prM-E may be explained by the low specific infectivity of particles encapsidated in DENV envelope protein (van der Schaar *et al.*, 2007; Winkelmann *et al.*, 2011), although we were unable to exclude the possibility that the viral assembly and/or secretion with dengue prM-E is not efficient (Chang *et al.*, 2003; Hsieh *et al.*, 2008). Adaptive mutations in structural and NS proteins could possibly enhance the production of infectious particles by improving the specific infectivity of the resulting particles (Winkelmann *et al.*, 2011). In addition, it has been reported that a chimaeric WNV genome with DENV2 prM-E genes but lacking the C gene replicates much better in DENV2-C-expressing cells than in WNV-C-expressing cells (Suzuki *et al.*, 2009), thus suggesting that the combination of homologous C protein and prM-E proteins improves the production of viral particles. Therefore, it is possible to obtain a better yield of dengue SRIPs by using DENV C protein instead of JEV C protein. Such DENV-SRIPs can be useful for studying infection-enhancing and neutralizing antibody activities.

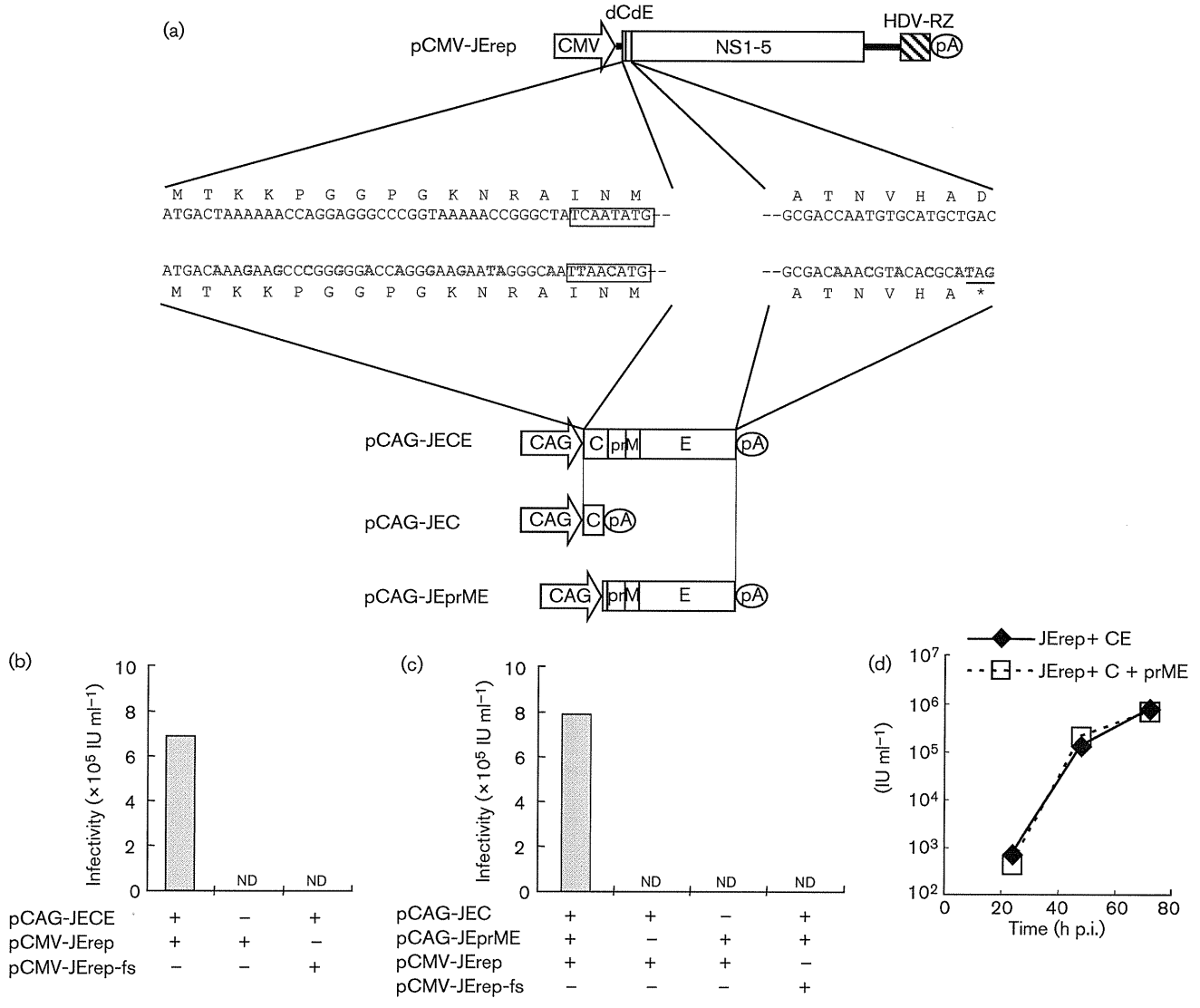

Fig. 2. Schematic representation of JEV replicon and structural protein-expression plasmids. (a) Top: JEV subgenomic replicon with deletion of structural proteins. This replicon contains a partial C and E gene. Bottom: JEV structural protein-expression plasmids showing the region of overlap with JEV replicon. Boxes indicate the 8 nt in the 5′ CS that are 100 % conserved among all mosquito-borne flaviviruses. The JEV C-E, C and prM-E coding sequences harbour silent mutations designed to prevent homologous recombinations that included two changes to the CS sequence, which must be 100 % complementary to the 3′ CS of JEV in order to permit genome replication. The termination codon is underlined. Nucleotide substitutions are shown in red. (b, c) Titres of JEV-SRIPs produced by transfection of 293T cells with replicon plasmid and structural protein-expression plasmids. Dilutions of supernatant collected at 3 days post-transfection were used to inoculate monolayers of Vero cells. Cells were fixed at 2 days post-infection and stained with anti-NS1 antibody. Stained cells were then counted to determine the titres (IU ml^{-1}) produced by transfections. ND, Not detected. (d) Time course of JEV SRIP production from transfected cells. At each time point, medium was removed and frozen for subsequent titration and fresh medium was added. JEV SRIP titres were determined by assaying infectivity in Vero cells.

The plasmid-based production system offers an advantage for vaccine production in terms of stability and safety, as this method is able to reduce the chance of mutations in the structural protein region, as well as the risk of infection when compared with live virus production. In addition, our replicon plasmids have the potential for application to DNA-based vaccines, as described previously (Cao *et al.*, 2011; Chang *et al.*, 2008; Huang *et al.*, 2012).

In conclusion, we established a DNA-based production system for SRIPs of flaviviruses. This system has potential value as a basic research and diagnostic tool, and could be used to enhance the safety of neutralization assay, as well as vaccine production.

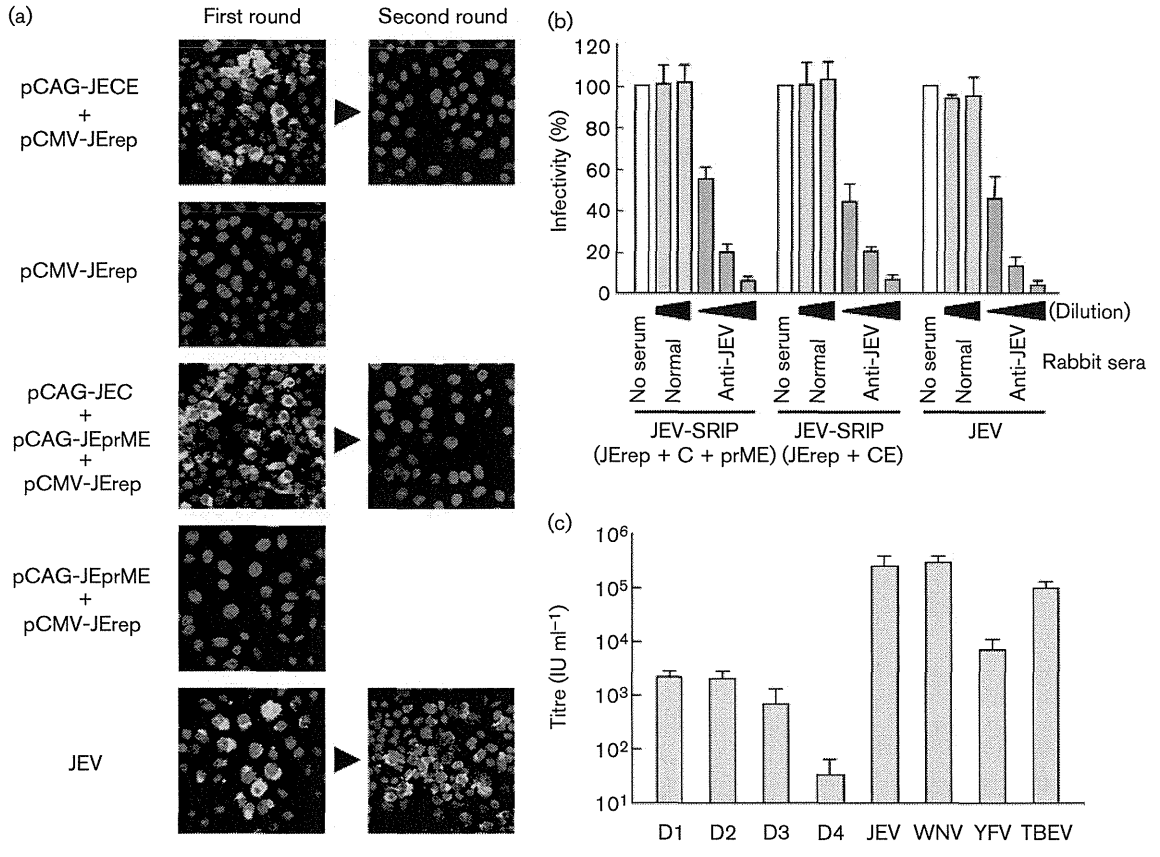

Fig. 3. Vero cells were inoculated with supernatant of 293T cells transfected with the indicated plasmids or infected with JEV. Two days post-inoculation, culture supernatants were collected, and cells were fixed and stained with NS1 antibodies (first round). Naive Vero cells were reinfected with culture supernatants from the first round. Two days post-inoculation, cells were fixed and stained with NS1 antibodies (second round). Cell nuclei were counterstained with DAPI. (b) JEV SRIP inoculum was incubated with serially diluted (1 : 2000, 1 : 8000 and 1 : 32 000) rabbit normal serum or anti-JEV serum for 1 h at room temperature, followed by inoculation onto Vero cells. Cells were immunostained with anti-NS1 antibody at 2 days post-infection, and antigen-positive cells were counted and used to calculate a titre based on f.f.u. ml^{-1} for spreading infections or IU ml^{-1} for non-spreading infections. Data for each condition are means of values obtained from three independent experiments with error bars showing SD. The value for controls without serum (no serum) was set at 100 %. (c) Infectious titres of flavivirus SRIPs, including dengue types 1–4 (D1–4), produced by transfection of 293T cells with pCMV-JErep, pCAG-JEC and flavivirus prM-E expression plasmids. Dilution of supernatant collected at 3 days post-transfection was used to inoculate monolayers of Vero cells. Cells were fixed at 2 days post-infection and stained with anti-JEV NS1 antibody, and stained cells were counted in order to determine titres.

Acknowledgements

The BIKEN Endowed Department of Dengue Vaccine Development, Faculty of Tropical Medicine, Mahidol University, Thailand, was endowed by the Research Foundation for Microbial Diseases of Osaka University, Osaka, Japan, to the Research Institute for Microbial Diseases, Osaka University, Osaka, Japan. We are grateful to K. Yoshii for providing the TBE structural protein-expression plasmid. We would also like to thank P. W. Mason, T. Kobayashi and T. Kato for their helpful discussions, as well as M. Sasaki and M. Yahata for technical assistance. This work was supported by Grants-in-Aid from the Ministry of Health, Labour and Welfare of Japan (H23-shinkou-ippan-010, H23-seisakutansaku-ippan-002). The authors declare no conflicts of interest.

References

Ansarah-Sobrinho, C., Nelson, S., Jost, C. A., Whitehead, S. S. & Pierson, T. C. (2008). Temperature-dependent production of pseudoinfectious dengue reporter virus particles by complementation. *Virology* **381**, 67–74.

Campbell, G. L., Hills, S. L., Fischer, M., Jacobson, J. A., Hoke, C. H., Hombach, J. M., Marfin, A. A., Solomon, T., Tsai, T. F. & other authors (2011). Estimated global incidence of Japanese encephalitis: a systematic review. *Bull World Health Organ* **89**, 766–774, 774A–774E.

Cao, F., Li, X. F., Yu, X. D., Deng, Y. Q., Jiang, T., Zhu, Q. Y., Qin, E. D. & Qin, C. F. (2011). A DNA-based West Nile virus replicon elicits humoral and cellular immune responses in mice. *J Virol Methods* **178**, 87–93.

Chang, G. J., Hunt, A. R., Holmes, D. A., Springfield, T., Chiueh, T. S., Roehrig, J. T. & Gubler, D. J. (2003). Enhancing biosynthesis and secretion of premembrane and envelope proteins by the chimeric plasmid of dengue virus type 2 and Japanese encephalitis virus. *Virology* **306**, 170–180.

Chang, D. C., Liu, W. J., Anraku, I., Clark, D. C., Pollitt, C. C., Suhrbier, A., Hall, R. A. & Khromykh, A. A. (2008). Single-round infectious particles enhance immunogenicity of a DNA vaccine against West Nile virus. *Nat Biotechnol* **26**, 571–577.

Gehrke, R., Ecker, M., Aberle, S. W., Allison, S. L., Heinz, F. X. & Mandl, C. W. (2003). Incorporation of tick-borne encephalitis virus replicons into virus-like particles by a packaging cell line. *J Virol* **77**, 8924–8933.

Hahn, C. S., Hahn, Y. S., Rice, C. M., Lee, E., Dalgarno, L., Strauss, E. G. & Strauss, J. H. (1987). Conserved elements in the 3′ untranslated region of flavivirus RNAs and potential cyclization sequences. *J Mol Biol* **198**, 33–41.

Hsieh, S. C., Liu, I. J., King, C. C., Chang, G. J. & Wang, W. K. (2008). A strong endoplasmic reticulum retention signal in the stem-anchor region of envelope glycoprotein of dengue virus type 2 affects the production of virus-like particles. *Virology* **374**, 338–350.

Huang, Y., Liu, S., Yang, P., Wang, C., Du, Y., Yu, W. & Sun, Z. (2012). Replicon-based Japanese encephalitis virus vaccines elicit immune response in mice. *J Virol Methods* **179**, 217–225.

Ishikawa, T., Takasaki, T., Kurane, I., Nukuzuma, S., Kondo, T. & Konishi, E. (2007). Co-immunization with West Nile DNA and inactivated vaccines provides synergistic increases in their immunogenicities in mice. *Microbes Infect* **9**, 1089–1095.

Jones, C. T., Patkar, C. G. & Kuhn, R. J. (2005). Construction and applications of yellow fever virus replicons. *Virology* **331**, 247–259.

Khromykh, A. A. & Westaway, E. G. (1997). Subgenomic replicons of the flavivirus Kunjin: construction and applications. *J Virol* **71**, 1497–1505.

Khromykh, A. A., Varnavski, A. N. & Westaway, E. G. (1998). Encapsidation of the flavivirus kunjin replicon RNA by using a complementation system providing Kunjin virus structural proteins in trans. *J Virol* **72**, 5967–5977.

Khromykh, A. A., Meka, H., Guyatt, K. J. & Westaway, E. G. (2001). Essential role of cyclization sequences in flavivirus RNA replication. *J Virol* **75**, 6719–6728.

Konishi, E., Shoda, M., Ajiro, N. & Kondo, T. (2004). Development and evaluation of an enzyme-linked immunosorbent assay for quantifying antibodies to Japanese encephalitis virus nonstructural 1 protein to detect subclinical infections in vaccinated horses. *J Clin Microbiol* **42**, 5087–5093.

Konishi, E., Kosugi, S. & Imoto, J. (2006). Dengue tetravalent DNA vaccine inducing neutralizing antibody and anamnestic responses to four serotypes in mice. *Vaccine* **24**, 2200–2207.

McAda, P. C., Mason, P. W., Schmaljohn, C. S., Dalrymple, J. M., Mason, T. L. & Fournier, M. J. (1987). Partial nucleotide sequence of the Japanese encephalitis virus genome. *Virology* **158**, 348–360.

Ng, C. Y., Gu, F., Phong, W. Y., Chen, Y. L., Lim, S. P., Davidson, A. & Vasudevan, S. G. (2007). Construction and characterization of a stable subgenomic dengue virus type 2 replicon system for antiviral compound and siRNA testing. *Antiviral Res* **76**, 222–231.

Pang, X., Zhang, M. & Dayton, A. I. (2001). Development of Dengue virus type 2 replicons capable of prolonged expression in host cells. *BMC Microbiol* **1**, 18.

Scholle, F., Girard, Y. A., Zhao, Q., Higgs, S. & Mason, P. W. (2004). *trans*-Packaged West Nile virus-like particles: infectious properties in vitro and in infected mosquito vectors. *J Virol* **78**, 11605–11614.

Shi, P. Y., Tilgner, M. & Lo, M. K. (2002). Construction and characterization of subgenomic replicons of New York strain of West Nile virus. *Virology* **296**, 219–233.

Sumiyoshi, H., Mori, C., Fuke, I., Morita, K., Kuhara, S., Kondou, J., Kikuchi, Y., Nagamatu, H. & Igarashi, A. (1987). Complete nucleotide sequence of the Japanese encephalitis virus genome RNA. *Virology* **161**, 497–510.

Suzuki, R., Winkelmann, E. R. & Mason, P. W. (2009). Construction and characterization of a single-cycle chimeric flavivirus vaccine candidate that protects mice against lethal challenge with dengue virus type 2. *J Virol* **83**, 1870–1880.

Suzuki, R., Matsuda, M., Watashi, K., Aizaki, H., Matsuura, Y., Wakita, T. & Suzuki, T. (2013). Signal peptidase complex subunit 1 participates in the assembly of hepatitis C virus through an interaction with E2 and NS2. *PLoS Pathog* **9**, e1003589.

van der Schaar, H. M., Rust, M. J., Waarts, B. L., van der Ende-Metselaar, H., Kuhn, R. J., Wilschut, J., Zhuang, X. & Smit, J. M. (2007). Characterization of the early events in dengue virus cell entry by biochemical assays and single-virus tracking. *J Virol* **81**, 12019–12028.

Winkelmann, E. R., Widman, D. G., Suzuki, R. & Mason, P. W. (2011). Analyses of mutations selected by passaging a chimeric flavivirus identify mutations that alter infectivity and reveal an interaction between the structural proteins and the nonstructural glycoprotein NS1. *Virology* **421**, 96–104.

Yoshii, K., Hayasaka, D., Goto, A., Obara, M., Araki, K., Yoshimatsu, K., Arikawa, J., Ivanov, L., Mizutani, T. & other authors (2003). Enzyme-linked immunosorbent assay using recombinant antigens expressed in mammalian cells for serodiagnosis of tick-borne encephalitis. *J Virol Methods* **108**, 171–179.

Yoshii, K., Goto, A., Kawakami, K., Kariwa, H. & Takashima, I. (2008). Construction and application of chimeric virus-like particles of tick-borne encephalitis virus and mosquito-borne Japanese encephalitis virus. *J Gen Virol* **89**, 200–211.

Yun, S. I., Song, B. H., Koo, Y., Jeon, I., Byun, S. J., Park, J. H., Joo, Y. S., Kim, S. Y. & Lee, Y. M. (2009). Japanese encephalitis virus-based replicon RNAs/particles as an expression system for HIV-1 $Pr55^{Gag}$ that is capable of producing virus-like particles. *Virus Res* **144**, 298–305.

Biochemical and Biophysical Research Communications 443 (2014) 808–813

Contents lists available at ScienceDirect

Biochemical and Biophysical Research Communications

journal homepage: www.elsevier.com/locate/ybbrc

Evaluation and identification of hepatitis B virus entry inhibitors using HepG2 cells overexpressing a membrane transporter NTCP ☆

Masashi Iwamoto [a,b], Koichi Watashi [a,b,*], Senko Tsukuda [a,c], Hussein Hassan Aly [a], Masayoshi Fukasawa [d], Akira Fujimoto [a], Ryosuke Suzuki [a], Hideki Aizaki [a], Takayoshi Ito [e], Osamu Koiwai [b], Hiroyuki Kusuhara [f], Takaji Wakita [a]

[a] Department of Virology II, National Institute of Infectious Diseases, Tokyo 162-8640, Japan
[b] Department of Applied Biological Science, Tokyo University of Sciences, Noda 278-8510, Japan
[c] Micro-signaling Regulation Technology Unit, RIKEN Center for Life Science Technologies, Wako 351-0198, Japan
[d] Department of Biochemistry and Cell Biology, National Institute of Infectious Diseases, Tokyo 162-8640, Japan
[e] Division of Gastroenterology, Department of Medicine, Showa University School of Medicine, Tokyo 142-8666, Japan
[f] The University of Tokyo, Graduate School of Pharmaceutical Sciences, Tokyo 113-0033, Japan

ARTICLE INFO

Article history:
Received 24 November 2013
Available online 14 December 2013

Keywords:
HBV
Infection
NTCP
DMSO
Cyclosporin
Oxysterol

ABSTRACT

Hepatitis B virus (HBV) entry has been analyzed using infection-susceptible cells, including primary human hepatocytes, primary tupaia hepatocytes, and HepaRG cells. Recently, the sodium taurocholate cotransporting polypeptide (NTCP) membrane transporter was reported as an HBV entry receptor. In this study, we established a strain of HepG2 cells engineered to overexpress the human NTCP gene (HepG2-hNTCP-C4 cells). HepG2-hNTCP-C4 cells were shown to be susceptible to infection by blood–borne and cell culture-derived HBV. HBV infection was facilitated by pretreating cells with 3% dimethyl sulfoxide permitting nearly 50% of the cells to be infected with HBV. Knockdown analysis suggested that HBV infection of HepG2-hNTCP-C4 cells was mediated by NTCP. HBV infection was blocked by an anti-HBV surface protein neutralizing antibody, by compounds known to inhibit NTCP transporter activity, and by cyclosporin A and its derivatives. The infection assay suggested that cyclosporin B was a more potent inhibitor of HBV entry than was cyclosporin A. Further chemical screening identified oxysterols, oxidized derivatives of cholesterol, as inhibitors of HBV infection. Thus, the HepG2-hNTCP-C4 cell line established in this study is a useful tool for the identification of inhibitors of HBV infection as well as for the analysis of the molecular mechanisms of HBV infection.

1. Introduction

Approximately 350 million people are estimated to be infected with hepatitis B virus (HBV) worldwide [1–4]. Chronically infected patients are at a greater risk of developing hepatocellular carcinoma. Currently, clinical treatment for HBV infection includes interferon (IFN)α and nucleos(t)ide analogs [2,4]. IFNα therapy yields long-term clinical benefit in less than 40% of the treated patients and can cause significant side effects. Nucleos(t)ide analog treatment can suppress HBV replication with substantial biochemical and histological improvement; however, such analogs may select drug-resistant viruses, thereby limiting the efficacy of long-term treatment. Thus, the development of new anti-HBV agents targeting a different molecule in the HBV life cycle is urgently needed.

HBV is a hepatotropic virus that mainly or exclusively infects human liver [1,5]. HBV infection can be reproduced in cell culture using primary human hepatocytes (PHH), primary tupaia hepatocytes (PTH), and HepaRG cells [6]. Although HBV infection into these cells is robust, these models have significant limitations as tools for analyzing the mechanisms of HBV infection. Notably, these models can yield unstable reproducibility among lots and low tolerability of transfection efficiency with plasmid and siRNA: preparation and culturing of these cells require significant

Abbreviations: Ab, antibody; cccDNA, covalently closed circular DNA; Cs, cyclosporin; DMSO, dimethyl sulfoxide; GEq, genome equivalent; HBc, HBV core protein; HBs, HBV surface protein; HBV, hepatitis B virus; NTCP, sodium taurocholate cotransporting polypeptide; OHC, hydroxycholesterol; PHH, primary human hepatocytes; PTH, primary tupaia hepatocytes.

* Corresponding author at: Department of Virology II, National Institute of Infectious Diseases, 1-23-1 Toyama, Shinjuku-ku, Tokyo 162-8640, Japan. Fax: +81 3 5285 1161.
E-mail address: kwatashi@nih.go.jp (K. Watashi).

0006-291X/$ - see front matter © 2013 The Authors. Published by Elsevier Inc. All rights reserved.
http://dx.doi.org/10.1016/j.bbrc.2013.12.052

technical skill. In the case of hepatitis C virus (HCV), development of the HCV cell culture (HCVcc) system, in which HCV produced from a JFH-1 strain-based molecular clone can reinfect Huh-7 cells, greatly contribute to the characterization of the HCV life cycle and the evaluation of novel anti-HCV drug candidates [7]. However, the above-noted limitations of HBV-susceptible cells have hampered analysis of the HBV life cycle and impeded identification of new anti-HBV drug targets. Thus, establishment of a novel cell line supporting HBV infection is expected to accelerate the molecular analyses of HBV infection as well as the development of anti-HBV agents.

Recently, the sodium taurocholate cotransporting polypeptide (NTCP) membrane transporter was reported as an HBV entry receptor [8]. NTCP is a sodium-dependent transporter for taurocholic acid, and belongs to a family of solute carrier proteins that consist of seven members (SLC10A1-A7) [9,10]. NTCP is expressed at the basolateral membrane of hepatocytes and mediates the transport of conjugated bile acids and some drugs from portal blood to the liver [11]. NTCP specifically interacts with the large surface protein of HBV, thereby functioning as a viral entry receptor [8].

In this study, we established a strain of HepG2 cells engineered to overexpress the NTCP-encoding gene. One of these clones, designated HepG2-hNTCP-C4, was shown to be highly susceptible for HBV infection, confirming that this infection is mediated by NTCP and permitting evaluation in these cells of the anti-HBV activity of various compounds: reduction of HBV infection of HepG2-hNTCP-C4 cells was observed upon treatment with compounds that blocked HBV entry in other assays and by known inhibitors of NTCP transporter activity [12]. A small-scale chemical screen permitted use to identify oxysterols as inhibitors of HBV infection. Thus, the cell line established in this study is useful for screening for anti-HBV agents, as well as for analysis of the molecular mechanisms of HBV infection.

2. Materials and methods

2.1. Reagents

Dimethyl sulfoxide (DMSO), anti-FLAG antibody (Ab), dextran sulfate, cholate, progesterone, 22(S)-hydroxycholesterol (OHC), 25-OHC, 20α-OHC, and 7β-OHC were purchased from Sigma. Ursodeoxycholate was purchased from Tokyo Chemical Industry. Bromosulfophthalein was from MP biomedicals. Cyclosporin (Cs)A, CsB, CsC, CsD, and CsH were obtained from Enzo Lifesciences. Anti-HBV surface protein (HBs) Ab was from Abcam. Heparin was obtained from Mochida Pharmaceuticals. Myrcludex-B was kindly provided by Dr. Stephan Urban at University Hospital Heidelberg and was synthesized by CS Bio (Shanghai, China).

2.2. Cell culture and plasmid transfection

HepG2 and HepG2-hNTCP-C4 cells were cultured with DMEM/F-12 + GlutaMax (Invitrogen) supplemented with 10 mM HEPES (Invitrogen), 200 units/ml penicillin, 200 μg/ml streptomycin, 10% FBS, 50 μM hydrocortisone and 5 μg/ml insulin in the presence (HepG2-hNTCP-C4 cells) or absence (HepG2 cells) of 400 μg/ml G418 (Nacalai). HepAD38 (kindly provided by Dr. Christoph Seeger at Fox Chase Cancer Center) [13] and HepaRG cells (BIOPREDIC) were cultured as described previously [14].

An expression plasmid for hNTCP [15] was transfected into HepG2 cells with TransIT-LT1 (Mirus) according to the manufacturer's instruction to establish HepG2-hNTCP-C4 cells.

2.3. HBV preparation and infection

HBV was prepared and infected as described [14]. Except as noted, the HBV used in this study was genotype D derived from HepAD38 cells [13]. HBV was infected into NTCP-expressing HepG2 cells at 6×10^3 or 1.8×10^4 genome equivalent (GEq)/cell or into HepaRG cells at 6×10^3 GEq/cell. All infections were performed in the presence of 4% PEG8000 at 37 °C for 16 h as previously described [14]. Dr. Urban's group reported that a quantity of more than 10^4 GEq/cell (i.e. $1.25 - 40 \times 10^4$ GEq/cell) of HBV derived from HepAD38 or HepG2.2.15 cells was required as an inoculum for efficient infection into HepaRG cells in the presence of 4% PEG8000 [16]. A limited number of infections were performed with HBV of genotype C, derived from the serum of an HBV-infected patient, at 100 GEq/cell.

2.4. Real-time PCR and RT-PCR

Real-time PCR for quantification of HBV covalently closed circular (ccc)DNA were performed as described [14]. Isolation of total RNA from cell lysates and reverse transcription PCR (RT-PCR) using a One step RNA PCR kit (Takara) were performed as described previously [17]. Primers used in this study were as follows: 5′-AGGGAGGAGGTGGCAATCAAGAGTGG-3′ and 5′-CCGGCTGAAGAACATTGAGGCACTGG-3′ for NTCP, 5′-CCATGGAGAAGGCTGGGG-3′ and 5′-CAAAGTTGTCATGGATGACC-3′ for GAPDH, respectively.

2.5. Detection of HBs and HBe antigens

HBs antigen was quantified by ELISA as described previously [14]. HBe antigen was detected by Chemiluminescent Immuno Assay (Mitsubishi Chemical Medience).

2.6. Southern blot analysis

Isolation of cellular DNA and southern blot analysis to detect HBV DNAs were performed as described previously [14].

2.7. Indirect immunofluorescence analysis

Immunofluorescence was conducted essentially as described [14] using an anti-HBc Ab (#B0586, DAKO) at a dilution of 1:1000.

2.8. Flow cytometry

An aliquot of 1×10^6 of HepG2 or HepG2-hNTCP-C4 cells was incubated for 30 min with a 1:50 dilution of anti-NTCP Ab (Abcam), then washed and incubated with a dye-labeled secondary Ab (Alexa Fluor 488, Invitrogen) at 1:500 dilution in the dark. Staining and washing were carried out at 4 °C in PBS supplemented with 0.5% bovine serum albumin and 0.1% sodium azide. The signals were analyzed with Cell Sorter SH8000 (SONY).

2.9. siRNA transfection

siRNAs were transfected into the cells at a final concentration of 10–30 nM using Lipofectamine RNAiMAX (Invitrogen) according to the manufacturer's protocol. siRNAs were purchased from Sigma.

2.10. Statistical analyses

Statistical analyses are done with student *t*-test.

3. Results and discussion

3.1. Establishment of a cell line susceptible to HBV infection

To establish a cell line permanently expressing NTCP, we transfected an NTCP-encoding plasmid into HepG2 cells and selected with G418 at 1 mg/ml for 3 weeks. The resultant 9 cell clones were isolated and NTCP expression was analyzed by RT-PCR. One of these clones, designated HepG2-hNTCP-C4, was used in the following experiments because this specific clone exhibited high expression of NTCP and high susceptibility to HBV infection, as shown below. Specifically, NTCP mRNA was abundantly expressed in HepG2-hNTCP-C4 cells, in contrast to little to no expression of NTCP mRNA in the parental HepG2 cells (Fig. 1A). Consistent with the mRNA levels, NTCP protein was detected on the cell surface in HepG2-hNTCP-C4 cells (Fig. 1B). To evaluate HBV infection, these cells were inoculated with HBV for 16 h and cultured in normal growth medium for an additional 12 days, and then HBV surface protein (HBs) and HBe antigens in the culture supernatant as well as HBV DNAs, covalently closed circular (ccc)DNA, and HBV core (HBc) in the cells were assessed. The HBV inoculum used in this experiment was of genotype D, and was derived from the culture supernatant of HepAD38 cells that produce HBV by depletion of tetracycline [13]. To confirm that the detected signals were derived from HBV infection and did not represent non-specific background, the cells were incubated with 1 μM Myrcludex-B (or with DMSO vehicle) for 3 h prior to and for 16 h during HBV infection. Myrcludex-B is a lipopeptide consisting of amino acid residues 2–48 of the pre-S1 region of HBV, and is known to block HBV entry [18]. Following HBV exposure, little or no HBs and HBe antigens was detected in the culture supernatant of the parental HepG2 cells, and little HBc protein was observed in these cells (Fig. 1C, D, and G). However, these proteins, as well as HBV DNAs and cccDNA, were detected in HBV-treated HepG2-hNTCP-C4 cells (Fig. 1C–G). The corresponding signals were significantly reduced in the cells treated with an HBV entry inhibitor, Myrcludex-B, but not in the cells treated with DMSO (Fig. 1C–G). These data suggested that HepG2-hNTCP-C4 cells are HBV-susceptible, in contrast to the parental HepG2 cells. The HepG2-hNTCP-C4 cell line also was susceptible to infection with HBV genotype C, which was derived from the serum of an HBV-infected patient (Fig. 1H and I).

3.2. HBV susceptibility of HepG2-hNTCP-C4 cells was augmented by pretreatment with DMSO

It has been reported that a prolonged HBV infection in primary human hepatocytes can be enhanced by pretreatment with DMSO [19]. Therefore, we examined whether pretreatment with DMSO affected HBV infection of HepG2-NTCP-C4 cells. The cells were pretreated with 3% DMSO for 24 h and then the HBV infectivity was investigated following the protocol as in Fig. 1. Immunofluorescence analysis revealed that approximately 50% of the DMSO-pretreated cells were HBc-positive at 12 days post-infection (Fig. 2A, middle), while only 10–20% of cells were HBc-positive cells in the absence of pretreatment (Fig. 1G, upper right). The effect of DMSO pretreatment on HBV susceptibility was both concentration-(Fig. 2B) and time-dependent (Fig. 2C).

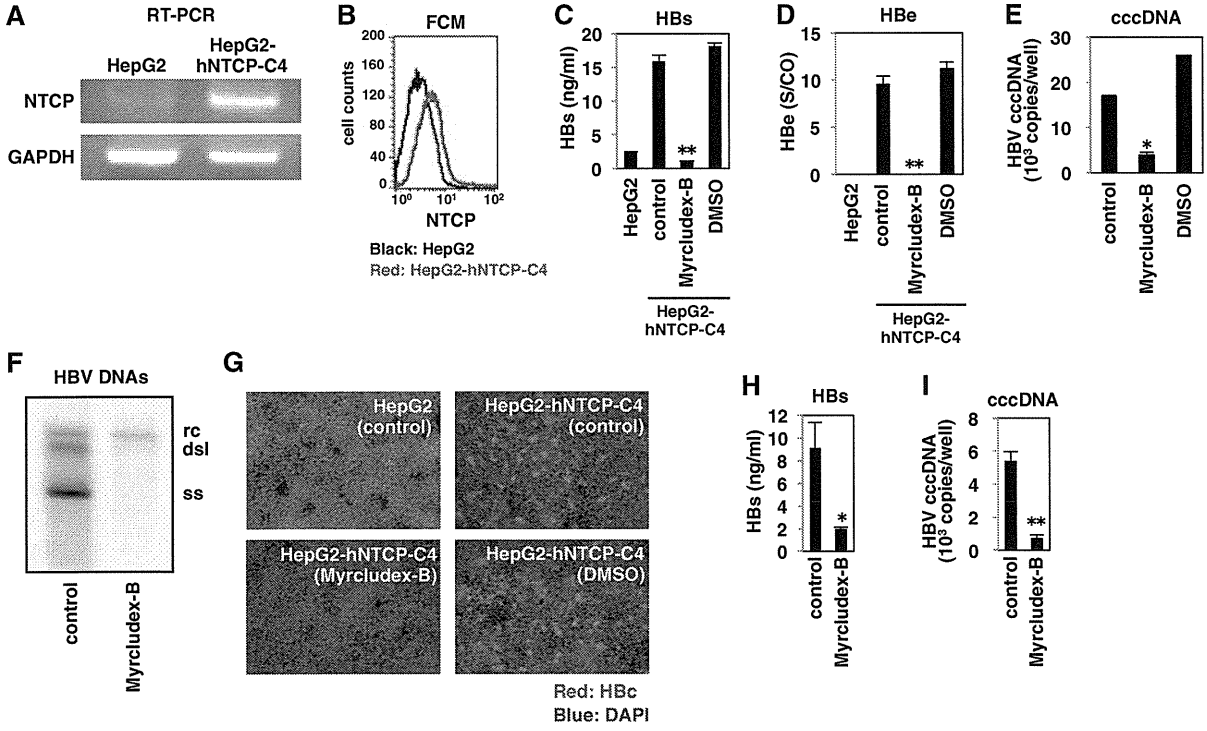

Fig. 1. Establishment of a cell line susceptible to hepatitis B virus (HBV) infection. (A) mRNAs for sodium taurocholate cotransporting polypeptide (NTCP) and GAPDH in HepG2 and HepG2-hNTCP-C4 cells were detected by RT-PCR. (B) NTCP protein on cell surface of HepG2 (black) and HepG2-hNTCP-C4 cells (red) was detected by flow cytometry. (C-G) HepG2-hNTCP-C4 or the parental HepG2 cells pretreated with or without 1 μM Myrcludex-B or vehicle (DMSO) for 3 h were inoculated with HBV (genotype D) for 16 h. After washing out of the free virus and the compounds, the cells were cultured for an additional 12 days in normal growth medium and then assayed for secretion of HBs (C) and HBe antigens (D) secreted in the culture supernatant, and for the presence of HBV covalently closed circular (ccc)DNA (E), HBV DNAs (F), and HBV core (HBc) proteins (G) in the cells. rc, dsl, and ss in (F) indicate relaxed circular, double strand linear, and single strand HBV DNA, respectively. Red and blue signals in (G) indicate HBc protein and nuclear staining, respectively. (H and I) Infection of blood–borne HBV into HepG2-hNTCP-C4 cells. HBV (genotype C) derived from an HBV-infected patient was used as an inoculum for the infection assay. Levels for HBs antigen in the culture supernatant (H) and HBV cccDNA in the cells (I) are shown. The data in C–E, H, and I show the means of three independent experiments. $^{*}P < 0.05$, $^{**}P < 0.01$.

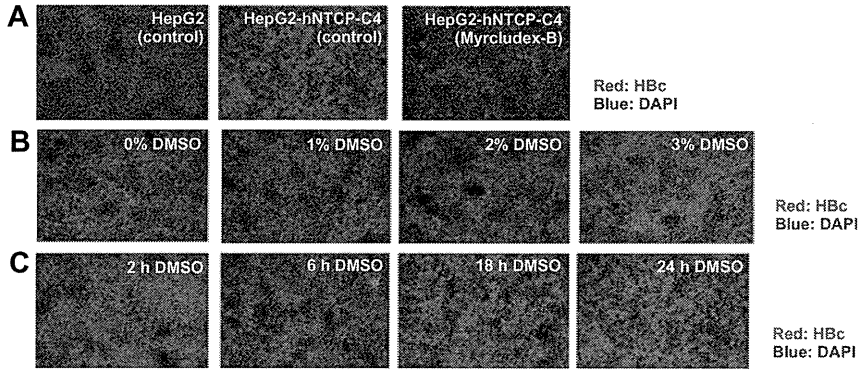

Fig. 2. HBV infection was facilitated by pretreatment of HepG2-hNTCP-C4 cells with DMSO. (A) HepG2 or HepG2-hNTCP-C4 cells preincubated with 3% DMSO for 24 h were inoculated with HBV in the presence of 3% DMSO for 16 h. Treatment with Myrcludex-B was used as a negative control for infection. At 12 days postinfection, HBc protein (red) and the nucleus (blue) were detected by immunofluorescence analysis. (B) Cells were pretreated by exposure for 24 h to various concentrations of DMSO (0–3%). (C) Cells were pretreated by exposure to 3% DMSO for various treatment times (2, 6, 18, and 24 h). HBc protein (red) and the nucleus (blue) were detected as in (A).

3.3. HBV infection was mediated by NTCP in HepG2-hNTCP-C4 cells

We used knockdown analysis to determine whether HBV infection of HepG2-hNTCP-C4 cells was mediated by NTCP. Transfection with siRNA against NTCP (si-NTCP) and GAPDH (si-GAPDH) specifically knocked down mRNA for NTCP and GAPDH, respectively, in HepG2-hNTCP-C4 cells (Fig. 3A). Consistent with the effect on transcript level, treatment with si-NTCP depleted NTCP protein on the cell surface (Fig. 3B). The HBV infection assay, performed as in Fig. 1, indicated that depletion of NTCP reduced the levels for HBs (Fig. 3C) and HBe antigens (Fig. 3D) in culture supernatant as well as HBV cccDNA (Fig. 3E) and HBc protein (Fig. 3F) in the cells at 12 days postinfection with HBV. These data suggested that HBV infection into HepG2-hNTCP-C4 cells was mediated by NTCP.

3.4. Evaluation of HBV entry inhibitors in HepG2-hNTCP-C4 cells

To determine whether HepG2-hNTCP-C4 cells could be used to evaluate anti-HBV activity of compounds, we examined the effect of known entry inhibitors in these cells. The cells were pretreated with compounds for 3 h and then inoculated with HBV for 16 h in the presence of compounds (Fig. 4A). Inoculation with HBV was followed by culturing of the cells in normal growth medium for an additional 12 days until detection of HBs antigen in the culture supernatant and cccDNA in the cells (Fig. 4A). This protocol has been used previously to evaluate the entry inhibition activity of compounds [20]. Treatment with anti-HBs neutralizing Ab, but not that with a non-relevant anti-FLAG Ab, inhibited HBV infection (Fig. 4B). Heparin and dextran sulfate, which have been reported to inhibit HBV attachment to the target cells [21], also reduced HBV infection (Fig. 4C). In addition, known NTCP substrates and inhibitors, including ursodeoxycholate, cholate, progesterone, and bromosulfophthalein [12], blocked HBV infection in this assay (Fig. 4D). We recently identified that cyclosporin A (CsA) and its analogs blocked HBV entry through inhibition of interaction between NTCP and the HBV large surface protein [20]. As shown in Fig. 4E, CsA and its analogs inhibited HBV infection in the present assay, with CsB showing the highest potency for inhibition of HBV infection among Cs analogs (Fig. 4E). These data indicate that HepG2-hNTCP-C4 cells are useful for evaluating the effect of HBV entry inhibitors.

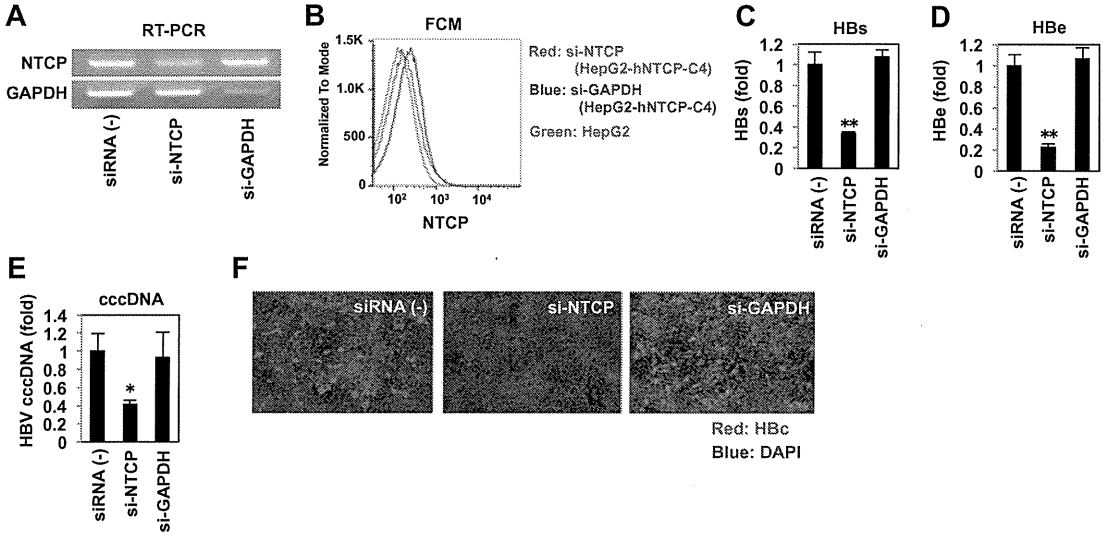

Fig. 3. HBV infection of HepG2-hNTCP-C4 cells was mediated by NTCP. (A) HepG2-hNTCP-C4 cells were transfected (for 48 h) with or without [siRNA(−)] siRNAs against NTCP (si-NTCP) or GAPDH (si-GAPDH), and mRNA expression levels of NTCP and GAPDH were detected by RT-PCR. (B) Parental HepG2 and HepG2-hNTCP-C4 cells were transfected (for 48 h) with or without si-NTCP or si-GAPDH, and cell surface-displayed NTCP protein was detected by flow cytometry. The red, blue, and green lines indicate the signal in HepG2-hNTCP-C4 cells treated with si-NTCP, HepG2-hNTCP-C4 cells treated with si-GAPDH, and HepG2 cells, respectively. (C–F) The cells prepared as in (A) were infected with HBV according to the protocol shown in Fig. 1. Culture supernatants were assayed for levels of secreted HBs (C) and HBe (D) antigens, and cells were assayed for intracellular levels of HBV cccDNA (E) and HBc protein (F). The red and blue signals in (F) indicate HBc and nuclear staining, respectively.

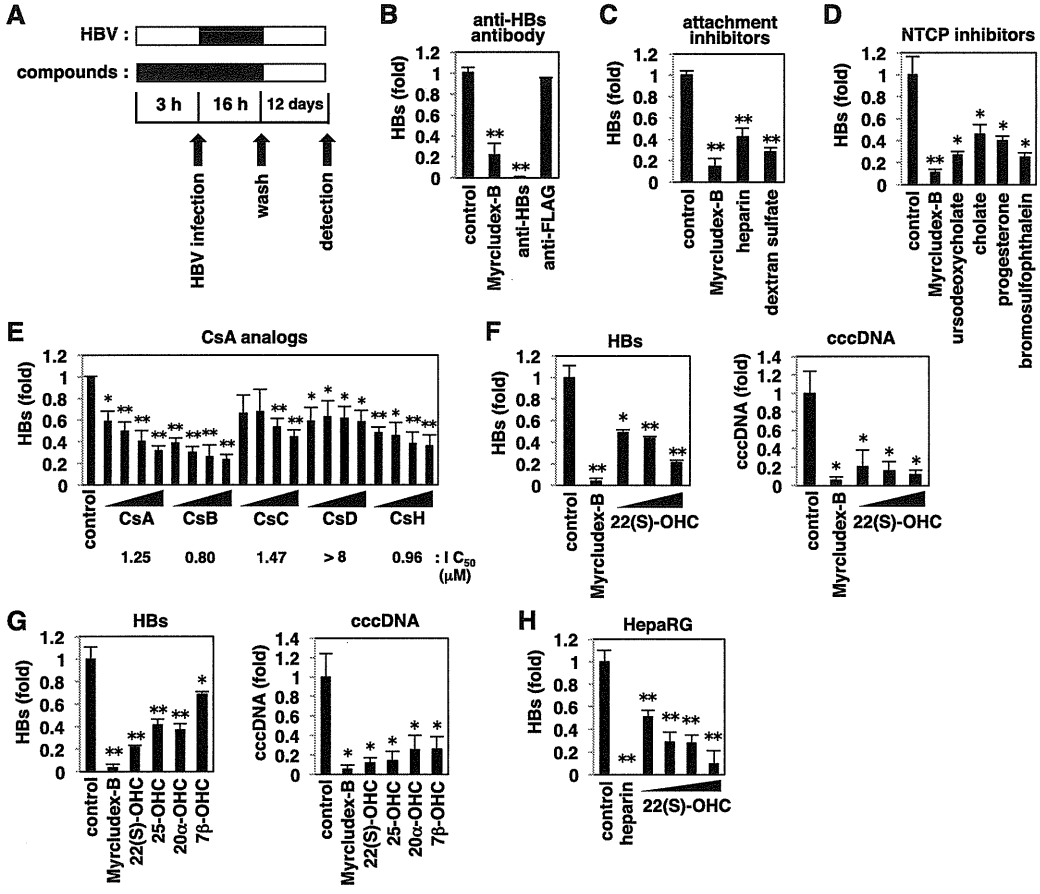

Fig. 4. Evaluation of HBV entry inhibitors in HepG2-hNTCP-C4 cells. (A) Schematic representation of the experimental procedure for evaluating HBV entry inhibition. HepG2-hNTCP-C4 cells were pretreated with or without compounds for 3 h and then inoculated with HBV for 16 h. After washing out of free HBV and the compounds, the cells were cultured with normal culture medium in the absence of compounds for an additional 12 days, and HBs antigen in the culture supernatant and/or HBV cccDNA in the cells were detected. Black and white bars show period of treatment and without treatment, respectively. (B–G) HepG2-hNTCP-C4 cells were treated with or without 1 μM Myrcludex-B, 10 μg/ml anti-HBs or anti-FLAG Ab (B); HBV attachment inhibitors including 100 IU/ml heparin and 1 mg/ml dextran sulfate (C); NTCP inhibitors including 100 μM ursodeoxycholate, 100 μM cholate, 40 μM progesterone, and 100 μM bromosulfophthalein (D); cyclosporins (CsA, CsB, CsC, CsD, CsH) at 1, 2, 4, and 8 μM (E); 22(S)-hydroxycholesterol (OHC) at 11, 33, and 100 μM (F); or oxysterols including 22(S)-OHC, 25-OHC, 20α-OHC, and 7β-OHC at 100 μM (G). For each assay, the cells were infected with HBV as shown in (A) and the levels of HBs antigen secreted into the culture supernatant and/or cccDNA in the cells were detected. Pretreatment time of compounds in (F) and (G) was 6 h, instead of 3 h. IC_{50}s of cyclosporin derivatives calculated in this assay are shown below the graph in (E). (H) HepaRG cells were treated with or without various concentrations of 22(S)-OHC (0.3, 0.9, 3, and 9 μM) and infected with HBV according to the protocol shown in (A). HBV infection was monitored by detecting the level of HBs secreted into the culture supernatant.

As there are only reverse transcriptase inhibitors currently available as anti-HBV drugs that inhibit the HBV life cycle, development of new anti-HBV agents targeting different steps in the HBV life cycle are greatly needed [1–4]. We therefore screened for compounds that blocked HBV entry by following the same protocol as in Fig. 4A. We found that an oxysterol, 22(S)-hydroxycholesterol (OHC), reduced HBV infection in a dose-dependent manner (Fig. 4F). Other oxysterols, 25-OHC, 20α-OHC, and 7β-OHC, also significantly decreased HBV infection (Fig. 4G). To validate this result, we repeated the assay using HepaRG cells, a line that frequently has been used in HBV entry experiments [14]. We found that 22(S)-OHC also reduced HBV infection of HepaRG cells in a dose-dependent manner (Fig. 4H), suggesting that the observed inhibitory effect of oxysterols reflects a genuine inhibition of HBV infection.

Thus, we have newly established a cell line that is susceptible to HBV infection. HepG2-hNTCP-C4 cells exhibited approximately 50% of HBV-infection positive cells (Fig. 2A), while maximum HBV infection of HepaRG cells was reported to be only 7% [16] or 20% [22] of the total population. These cells are expected to be useful for analyzing the molecular mechanisms of HBV infection, given that HepG2-derived cells show higher efficiency of transfection with expression plasmids and siRNAs than the current available HBV-susceptible PHH, PTH, and HepaRG cells. HepG2-hNTCP-C4 cells will facilitate knockdown analysis of host factors to define their roles in infection and screenings of compounds to identify novel inhibitors of HBV infection. As an example, we demonstrated here that oxysterols blocked HBV infection. The molecular mechanisms whereby oxysterols inhibit HBV infection are now under investigation. These analyses will be important for understanding the mechanisms of HBV infection as well as for developing new anti-HBV agents.

Acknowledgments

HepAD38 cells were kindly provided by Dr. Christoph Seeger at Fox Chase Cancer Center. Myrcludex-B, a pre-S1 lipopeptide, was kindly provided by Dr. Stephan Urban at University Hospital Heidelberg. We also are grateful to all of the members of Department of Virology II, National Institute of Infectious Diseases. This study was supported by Grants-in-aid from the Ministry of Health, Labor, and Welfare, Japan, from the Ministry of Education, Culture, Sports, Science, and Technology, Japan, and from Japan Society for the Promotion of Science, and from the Research on Health Sciences Focusing on Drug Innovation from the Japan Health Sciences Foundation.

References

[1] D. Grimm, R. Thimme, H.E. Blum, HBV life cycle and novel drug targets, Hepatol. Int. 5 (2011) 644–653.

[2] J.M. Pawlotsky, G. Dusheiko, A. Hatzakis, D. Lau, G. Lau, T.J. Liang, S. Locarnini, P. Martin, D.D. Richman, F. Zoulim, Virologic monitoring of hepatitis B virus therapy in clinical trials and practice: recommendations for a standardized approach, Gastroenterology 134 (2008) 405–415.

[3] M. Rapicetta, C. Ferrari, M. Levrero, Viral determinants and host immune responses in the pathogenesis of HBV infection, J. Med. Virol. 67 (2002) 454–457.

[4] F. Zoulim, Hepatitis B virus resistance to antiviral drugs: where are we going?, Liver Int 31 (Suppl. 1) (2011) 111–116.

[5] P. Gripon, S. Rumin, S. Urban, J. Le Seyec, D. Glaise, I. Cannie, C. Guyomard, J. Lucas, C. Trepo, C. Guguen-Guillouzo, Infection of a human hepatoma cell line by hepatitis B virus, Proc. Natl. Acad. Sci. USA 99 (2002) 15655–15660.

[6] D. Glebe, S. Urban, Viral and cellular determinants involved in hepadnaviral entry, World J. Gastroenterol. 13 (2007) 22–38.

[7] J.M. Gottwein, J. Bukh, Cutting the gordian knot-development and biological relevance of hepatitis C virus cell culture systems, Adv. Virus Res. 71 (2008) 51–133.

[8] H. Yan, G. Zhong, G. Xu, W. He, Z. Jing, Z. Gao, Y. Huang, Y. Qi, B. Peng, H. Wang, L. Fu, M. Song, P. Chen, W. Gao, B. Ren, Y. Sun, T. Cai, X. Feng, J. Sui, W. Li, Sodium taurocholate cotransporting polypeptide is a functional receptor for human hepatitis B and D virus, Elife 1 (2012) e00049.

[9] M.S. Anwer, B. Stieger, Sodium-dependent bile salt transporters of the SLC10A transporter family: more than solute transporters, Pflugers Arch. (2013) (Epub ahead of print).

[10] P.J. Meier, B. Stieger, Bile salt transporters, Annu. Rev. Physiol. 64 (2002) 635–661.

[11] C. Seeger, W.S. Mason, Sodium-dependent taurocholic cotransporting polypeptide: a candidate receptor for human hepatitis B virus, Gut 62 (2013) 1093–1095.

[12] R.B. Kim, B. Leake, M. Cvetkovic, M.M. Roden, J. Nadeau, A. Walubo, G.R. Wilkinson, Modulation by drugs of human hepatic sodium-dependent bile acid transporter (sodium taurocholate cotransporting polypeptide) activity, J. Pharmacol. Exp. Ther. 291 (1999) 1204–1209.

[13] S.K. Ladner, M.J. Otto, C.S. Barker, K. Zaifert, G.H. Wang, J.T. Guo, C. Seeger, R.W. King, Inducible expression of human hepatitis B virus (HBV) in stably transfected hepatoblastoma cells: a novel system for screening potential inhibitors of HBV replication, Antimicrob. Agents Chemother. 41 (1997) 1715–1720.

[14] K. Watashi, G. Liang, M. Iwamoto, H. Marusawa, N. Uchida, T. Daito, K. Kitamura, M. Muramatsu, H. Ohashi, T. Kiyohara, R. Suzuki, J. Li, S. Tong, Y. Tanaka, K. Murata, H. Aizaki, T. Wakita, Interleukin-1 and tumor necrosis factor-alpha trigger restriction of hepatitis B virus infection via a cytidine deaminase activation-induced cytidine deaminase (AID), J. Biol. Chem. 288 (2013) 31715–31727.

[15] S. Mita, H. Suzuki, H. Akita, H. Hayashi, R. Onuki, A.F. Hofmann, Y. Sugiyama, Inhibition of bile acid transport across Na+/taurocholate cotransporting polypeptide (SLC10A1) and bile salt export pump (ABCB 11)-coexpressing LLC-PK1 cells by cholestasis-inducing drugs, Drug Metab. Dispos. 34 (2006) 1575–1581.

[16] A. Schulze, K. Mills, T.S. Weiss, S. Urban, Hepatocyte polarization is essential for the productive entry of the hepatitis B virus, Hepatology 55 (2012) 373–383.

[17] M. Koyanagi, M. Hijikata, K. Watashi, O. Masui, K. Shimotohno, Centrosomal P4.1-associated protein is a new member of transcriptional coactivators for nuclear factor-kappaB, J. Biol. Chem. 280 (2005) 12430–12437.

[18] P. Gripon, I. Cannie, S. Urban, Efficient inhibition of hepatitis B virus infection by acylated peptides derived from the large viral surface protein, J. Virol. 79 (2005) 1613–1622.

[19] P. Gripon, C. Diot, A. Corlu, C. Guguen-Guillouzo, Regulation by dimethylsulfoxide, insulin, and corticosteroids of hepatitis B virus replication in a transfected human hepatoma cell line, J. Med. Virol. 28 (1989) 193–199.

[20] K. Watashi, A. Sluder, T. Daito, S. Matsunaga, A. Ryo, S. Nagamori, M. Iwamoto, S. Nakajima, S. Tsukuda, K. Borroto-Esoda, M. Sugiyama, Y. Tanaka, Y. Kanai, H. Kusuhara, M. Mizokami, T. Wakita, Cyclosporin A and its analogs inhibit hepatitis B virus entry into cultured hepatocytes through targeting a membrane transporter NTCP, Hepatology, in press.

[21] A. Schulze, P. Gripon, S. Urban, Hepatitis B virus infection initiates with a large surface protein-dependent binding to heparan sulfate proteoglycans, Hepatology 46 (2007) 1759–1768.

[22] O. Hantz, R. Parent, D. Durantel, P. Gripon, C. Guguen-Guillouzo, F. Zoulim, Persistence of the hepatitis B virus covalently closed circular DNA in HepaRG human hepatocyte-like cells, J. Gen. Virol. 90 (2009) 127–135.